Table 2
The prevalence of HPV DNA in lung tumors with and without EGFR mutations.

Histology	EGFR mutations	HPV+/total	P-Value[a]
All	Exon 19 deletion		0.077
	Mutated	3/7 (43%)	
	Wild type	4/35 (11%)	
All	Exon 21 L858R		0.257
	Mutated	2/6 (33%)	
	Wild type	5/36 (14%)	
All	Either in exons 19/21		0.021
	Mutated	5/13 (38%)	
	Wild type	2/29 (7%)	
Adenocarcinomas	Either in exons 19/21		0.014
	Mutated	4/10 (40%)	
	Wild type	0/16 (0%)	
Squamous cell carcinomas	Either in exons 19/21		0.318
	Mutated	1/2 (50%)	
	Wild type	1/10 (10%)	

[a] P-Values were obtained by Fisher's exact test.

highest in exon 19 deletions (81%) followed by exon 21 L858R (71%) [17]. In this study, the response rate to gefitinib was not able to evaluate because all subjects were primary lung cancer and underwent surgery without gefitinib administration. In the previous study, however, all cases with HPV-16 integrated form were responsive to gefitinib [6]. These findings suggest a possible association between HPV-16 integration and exon 19 deletion although the sample size was too small to draw a conclusion.

HPV-58, a high-risk type of HPV, was detected in two cases but this type was not observed in our previous study [6]. A possible explanation is the difference in the version of INNO-LiPA HPV Genotyping kits between the present and previous studies, in which INNO-LiPA HPV Genotyping CE test and INNO-LiPA HPV Genotyping v2 test was used [6], respectively. It is quite likely that the sensitivity and specificity of the recent kit is improved. Although a false-positive detection of HPV-58 might be concerned, a significant association between HPV presence and EGFR mutations remained ($P=0.026$) even these two cases were counted as HPV-negative cases.

EGFR mutations in the normal respiratory epithelium were frequently found in patients with EGFR mutant ACs (43%) but not in wild-type tumors [18], which indicate that EGFR mutations are an early event in the pathogenesis of lung ACs. Frequent EGFR mutations in smaller tumors and tumors without lymph node metastasis were consistent with this hypothesis (Table 1). Regarding HPV DNA in the normal lung tissue, the HPV absence in normal lung tissue surrounding the HPV-positive tumors was reported [5,19], suggesting that lung carcinomas with EGFR mutations may be susceptible to HPV infection.

Both EGFR mutations and HPV detection were more frequently observed in Asian lung cancer patients than non-Asian patients [17,20], except Finland. Relatively higher HPV presence (33%, 4/12) and EGFR mutations (11%, 8/73) were reported in Finnish lung ACs [20,21]. Thus, HPV-positive lung ACs may share the ethnic/geographical distribution with lung ACs with EGFR mutations. In non-far-East Asian countries, on the other hand, predominant HPV detections in SQCs of the lung, rather than ACs, were reported [4,22]. Further studies are required to clarify the difference in the etiological role of HPV between, potentially, EGFR-mutation-related lung ACs and SQCs from non-far-East Asian countries.

Wu et al. [14] demonstrated that HPV-16 E6 upregulated cIAP2, cellular inhibitor of apoptosis 2, via EGFR/PI3K/AKT cascade, and cIAP2 expression was positively related to EGFR mutations. Since the activation of PI3-kinase signaling was essential for HPV-induced transformation [23], the EGFR/PI3K/AKT cascade may play a pivotal role in carcinogenesis of HPV-related lung cancer with EGFR mutations.

The low viral load, as observed in the present study, casts doubt on the etiological role of HPV in lung carcinogenesis. However, the low viral load may be sufficient if HPV infection targets on cancer stem cells. Another possible explanation is the chromosomal instability induced by high-risk HPV E6-E7, leading to a selective growth advantage of malignant cells [24,25].

The transmission route of HPV in lung tumors is yet unclear. HPV detection in cancers of the oral cavity and oropharynx suggested a possibility of sexual transmission [26], indicating HPV infection of the lung through the upper aero-digestive tract. Another possible explanation is that there might be the transmission via the air stream carrying infected cell complexes or particles to the periphery of the lung [3].

The origins of lung ACs arising in smokers and never-smokers might travel down different pathways [27]. Tobacco-related carcinogens favor KRAS mutations in smokers, while unidentified carcinogens induce EGFR mutations in never-smokers. EGFR mutations predominantly activated phosphorylated AKT-mediated downstream pathways, rather than phosphorylated MAPK-mediated ones [28]. Thus, never-smokers may have distinct characters dependent on more simple signaling pathways like EGFR/AKT for survival of tumor cells.

In conclusion, the present study suggests a significant association between high-risk type HPVs and EGFR mutations in Japanese patients with lung cancer. The EGFR/PI3K/AKT cascade may play a pivotal role in carcinogenesis of HPV-related lung cancer with EGFR mutations.

Conflict of interest

None declared.

Acknowledgements

This study was supported by Grants-in-Aid for Scientific Research on Priority Areas (17015037) of the Ministry of Education, Culture, Sports, Science and Technology, Japan. We thank Ms. Yoshie Minakami for excellent technical work and Joint Research Laboratory, Kagoshima University Graduate School of Medical and Dental Sciences, for the use of their facilities.

Appendix A. Supplementary data

Supplementary data associated with this article can be found, in the online version, at doi:10.1016/j.lungcan.2012.08.011.

References

[1] Durst M, Gissmann L, Ikenberg H, zur Hausen H. A papillomavirus DNA from a cervical carcinoma and its prevalence in cancer biopsy samples from different geographic regions. Proc Natl Acad Sci USA 1983;80:3812–5.
[2] Human papillomaviruses. IARC Monogr Eval Carcinog Risks Hum 2007;90:476–7.
[3] Klein F, Amin Kotb WF, Petersen I. Incidence of human papilloma virus in lung cancer. Lung Cancer 2009;65:13–8.
[4] Aguayo F, Castillo A, Koriyama C, Higashi M, Itoh T, Capetillo M, et al. Human papillomavirus-16 is integrated in lung carcinomas: a study in Chile. Br J Cancer 2007;97:85–91.
[5] Cheng YW, Chiou HL, Sheu GT, Hsieh LL, Chen JT, Chen CY, et al. The association of human papillomavirus 16/18 infection with lung cancer among nonsmoking Taiwanese women. Cancer Res 2001;61:2799–803.
[6] Baba M, Castillo A, Koriyama C, Yanagi M, Matsumoto H, Natsugoe S, et al. Human papillomavirus is frequently detected in gefitinib-responsive lung adenocarcinomas. Oncol Rep 2010;23:1085–92.
[7] Paez JG, Janne PA, Lee JC, Tracy S, Greulich H, Gabriel S, et al. EGFR mutations in lung cancer: correlation with clinical response to gefitinib therapy. Science 2004;304:1497–500.

[8] Lynch TJ, Bell DW, Sordella R, Gurubhagavatula S, Okimoto RA, Brannigan BW, et al. Activating mutations in the epidermal growth factor receptor underlying responsiveness of non-small-cell lung cancer to gefitinib. N Engl J Med 2004;350:2129–39.
[9] Mitsudomi T, Kosaka T, Yatabe Y. Biological and clinical implications of EGFR mutations in lung cancer. Int J Clin Oncol 2006;11:190–8.
[10] Kleter B, van Doorn LJ, ter Schegget J, Schrauwen L, van Krimpen K, Burger M, et al. Novel short-fragment PCR assay for highly sensitive broad-spectrum detection of anogenital human papillomaviruses. Am J Pathol 1998;153:1731–9.
[11] Peitsaro P, Johansson B, Syrjanen S. Integrated human papillomavirus type 16 is frequently found in cervical cancer precursors as demonstrated by a novel quantitative real-time PCR technique. J Clin Microbiol 2002;40:886–91.
[12] Sharma SV, Bell DW, Settleman J, Haber DA. Epidermal growth factor receptor mutations in lung cancer. Nat Rev Cancer 2007;7:169–81.
[13] Sugio K, Uramoto H, Ono K, Oyama T, Hanagiri T, Sugaya M, et al. Mutations within the tyrosine kinase domain of EGFR gene specifically occur in lung adenocarcinoma patients with a low exposure of tobacco smoking. Br J Cancer 2006;94:896–903.
[14] Wu HH, Wu JY, Cheng YW, Chen CY, Lee MC, Goan YG, et al. cIAP2 upregulated by E6 oncoprotein via epidermal growth factor receptor/phosphatidylinositol 3-kinase/AKT pathway confers resistance to cisplatin in human papillomavirus 16/18-infected lung cancer. Clin Cancer Res 2010;16:5200–10.
[15] Arias-Pulido H, Joste N, Chavez A, Muller CY, Dai D, Smith HO, et al. Absence of epidermal growth factor receptor mutations in cervical cancer. Int J Gynecol Cancer 2008;18:749–57.
[16] Na II, Kang HJ, Cho SY, Koh JS, Lee JK, Lee BC, et al. EGFR mutations and human papillomavirus in squamous cell carcinoma of tongue and tonsil. Eur J Cancer 2007;43:520–6.
[17] Mitsudomi T, Yatabe Y. Mutations of the epidermal growth factor receptor gene and related genes as determinants of epidermal growth factor receptor tyrosine kinase inhibitors sensitivity in lung cancer. Cancer Sci 2007;98:1817–24.
[18] Tang X, Shigematsu H, Bekele BN, Roth JA, Minna JD, Hong WK, et al. EGFR tyrosine kinase domain mutations are detected in histologically normal respiratory epithelium in lung cancer patients. Cancer Res 2005;65:7568–72.
[19] Ciotti M, Giuliani L, Ambrogi V, Ronci C, Benedetto A, Mineo TC, et al. Detection and expression of human papillomavirus oncogenes in non-small cell lung cancer. Oncol Rep 2006;16:183–9.
[20] Chen YC, Chen JH, Richard K, Chen PY, Christiani DC. Lung adenocarcinoma and human papillomavirus infection. Cancer 2004;101:1428–36.
[21] Sihto H, Puputti M, Pulli L, Tynninen O, Koskinen W, Aaltonen LM, et al. Epidermal growth factor receptor domain II, IV, and kinase domain mutations in human solid tumors. J Mol Med (Berl) 2005;83:976–83.
[22] Yousem SA, Ohori NP, Sonmez-Alpan E. Occurrence of human papillomavirus DNA in primary lung neoplasms. Cancer 1992;69:693–7.
[23] Henken FE, Banerjee NS, Snijders PJ, Meijer CJ, De-Castro Arce J, Rosl F, et al. PIK3CA-mediated PI3-kinase signalling is essential for HPV-induced transformation in vitro. Mol Cancer 2011;10:71.
[24] Vinokurova S, Wentzensen N, Kraus I, Klaes R, Driesch C, Melsheimer P, et al. Type-dependent integration frequency of human papillomavirus genomes in cervical lesions. Cancer Res 2008;68:307–13.
[25] Masuda A, Takahashi T. Chromosome instability in human lung cancers: possible underlying mechanisms and potential consequences in the pathogenesis. Oncogene 2002;21:6884–97.
[26] Smith EM, Ritchie JM, Summersgill KF, Klussmann JP, Lee JH, Wang D, et al. Age, sexual behavior and human papillomavirus infection in oral cavity and oropharyngeal cancers. Int J Cancer 2004;108:766–72.
[27] Gazdar AF, Shigematsu H, Herz J, Minna JD. Mutations and addiction to EGFR: the Achilles 'heal' of lung cancers? Trends Mol Med 2004;10:481–6.
[28] Hosokawa S, Toyooka S, Fujiwara Y, Tokumo M, Soh J, Takigawa N, et al. Comprehensive analysis of EGFR signaling pathways in Japanese patients with non-small cell lung cancer. Lung Cancer 2009;66:107–13.

Clinical Study

Oncology

Oncology 2012;83:158–164
DOI: 10.1159/000341390

Received: May 9, 2012
Accepted after revision: June 22, 2012
Published online: August 7, 2012

Expression of Stanniocalcin 1 as a Potential Biomarker of Gastric Cancer

Takaaki Arigami[a, b] Yoshikazu Uenosono[b] Sumiya Ishigami[a]
Takahiko Hagihara[a] Naoto Haraguchi[a] Daisuke Matsushita[a]
Shigehiro Yanagita[a] Akihiro Nakajo[a] Hiroshi Okumura[a] Shuichi Hokita[c]
Shoji Natsugoe[a, b]

[a]Department of Digestive Surgery, Breast and Thyroid Surgery, Field of Oncology, [b]Molecular Frontier Surgery, Course of Advanced Therapeutics, Graduate School of Medical and Dental Sciences, Kagoshima University, and [c]Department of Surgery, Jialkai Imamura Hospital, Kagoshima, Japan

Key Words
Blood marker · Gastric cancer · Stanniocalcin 1 · Reverse transcription-polymerase chain reaction · Tumor progression

Abstract
Objective: We investigated stanniocalcin 1 (STC 1) expression to assess its clinical utility as a blood marker in patients with gastric cancer and evaluated its biological impact in terms of tumor aggressiveness. ***Methods:*** Blood specimens from 93 patients with gastric cancer and 21 normal healthy volunteers were assessed by quantitative reverse transcription-polymerase chain reaction for STC 1 mRNA expression. ***Results:*** The relative numbers of STC 1 mRNA copies were significantly higher in gastric cancer cell lines and in blood specimens from patients with gastric cancer than in blood specimens from healthy volunteers ($p = 0.0001$ and $p = 0.003$, respectively). The sensitivity and specificity of STC 1 mRNA expression for discriminating patients with gastric cancer from healthy volunteers were 69.9 and 71.4%, respectively. Furthermore, the sensitivity for STC 1 mRNA was higher than that for serum carcinoembryonic antigen and carbohydrate antigen 19-9. The presence of STC 1 expression was significantly correlated with depth of tumor invasion and tumor stage ($p = 0.032$ and $p = 0.013$, respectively). ***Conclusion:*** Our data strongly suggest that STC 1 is a potentially useful blood marker for predicting biological tumor aggressiveness in patients with gastric cancer.

Introduction

Gastric cancer is one of the most common malignant neoplasms in Japan [1]. In the last decade, the prognosis of patients with unresectable advanced or recurrent gastric cancer has dramatically improved due to the advance of anticancer agents, including novel molecular-targeted drugs such as trastuzumab [2–5]. Furthermore, the 5-year survival rate in patients with resectable advanced gastric cancer has been raised by a combination of curative surgery with D2 lymphadenectomy and adjuvant chemotherapy with S-1 [3]. However, some postoperative patients have a high risk of disease recurrence. Additionally, it is hard to predict patients at increased risk of

KARGER
Fax +41 61 306 12 34
E-Mail karger@karger.ch
www.karger.com

0030–2414/12/0833–0158$38.00/0

Accessible online at:
www.karger.com/ocl

Takaaki Arigami, MD, PhD
Department of Digestive Surgery, Field of Oncology, Molecular Frontier Surgery
Course of Advanced Therapeutics, Graduate School of Medical and Dental Sciences
Kagoshima University, 8-35-1 Sakuragaoka, Kagoshima 890-8520 (Japan)
Tel. +81 99 275 5361, E-Mail arigami@m.kufm.kagoshima-u.ac.jp

postoperative disease recurrence. Several investigators have demonstrated the clinical impact of circulating tumor cells (CTC) as an underlying cause of disease recurrence [6–9]. At present, carcinoembryonic antigen (CEA) and carbohydrate antigen 19-9 (CA 19-9) are clinically utilized to monitor CTC as conventional blood markers in patients with gastric cancer. Unfortunately, the sensitivity and specificity of these blood markers are not sufficient to discriminate patients with gastric cancer from healthy controls and to detect subclinical patients with a potential risk of recurrence. Moreover, it is problematic that promising blood markers for patients with gastric cancer are limited in clinical management.

Stanniocalcin (STC) was initially discovered in the corpuscles of Stannius of bony fish; it controls calcium and phosphate homeostasis to prevent hypercalcemia [10–15]. STC 1 is one of the STC family members, and a human cDNA clone encoding the mammalian homolog of STC was first isolated in 1996 [11]. The human STC 1 gene consists of 4 exons, spans 13 kb and is mapped to 8p11.2–p21. Previous studies have demonstrated that STC 1 is involved in various biological mechanisms of tumor progression [16–20]. Furthermore, STC 1 enhances tumor angiogenesis via up-regulation of vascular endothelial growth factor (VEGF) [18]. STC 1 is overexpressed in primary tumor cells of several malignancies, such as carcinomas of the esophagus, stomach, colorectum, breast, lung and ovary [17–19, 21–24]. However, little is understood about the clinical significance of STC 1 expression in blood specimens from patients with gastric cancer.

The purpose of the present study was to investigate STC 1 expression in blood specimens from patients with gastric cancer and to compare the clinical utility of STC 1 with those of conventional serum markers for cancer detection. Additionally, we assessed the relationship between STC 1 expression and clinicopathological features of patients with gastric cancer.

Materials and Methods

Gastric Cancer Cell Lines

Five gastric cancer cell lines (MKN-7, MKN-45, MKN-74, KATO-III and NUGC-4) were cultured in RPMI 1640 (Nissui Pharmaceutical Co., Ltd., Tokyo, Japan) supplemented with 10% fetal calf serum (Mitsubishi Kasei, Tokyo, Japan), 100 U/ml penicillin and 100 U/ml streptomycin. All cancer cell lines were incubated at 37°C in a humidified atmosphere containing 5% CO_2, as described previously [25, 26]. These cell lines were used for reverse transcription-polymerase chain reaction (RT-PCR).

Patients

In the present study, blood specimens were preoperatively collected from 93 patients (64 men and 29 women; age range, 35–87 years; average, 68 years) with gastric cancer who underwent curative gastrectomy with lymphadenectomy at the Kagoshima University Hospital (Kagoshima, Japan) between 2003 and 2005. Patients who received endoscopic treatment, palliative resection, preoperative chemotherapy, and/or radiotherapy were excluded from this study. The study patients were classified and staged on the basis of criteria for the tumor-node-metastasis classification of gastric carcinoma established by the UICC (International Union Against Cancer) [27]. Normal peripheral blood lymphocytes (PBLs) obtained and isolated from 21 healthy volunteers without cancer were used as a control. Moreover, we collected 20 surgical paraffin-embedded archival tissue (PEAT) specimens of resected primary tumor sites from patients enrolled in this study and these PEAT specimens were used for immunohistochemistry (IHC).

All patients provided written, informed consent to specimen collection in accordance with our institutional guidelines.

Enzyme Immunoassay Analysis for the Determination of Serum CEA and CA 19-9

Serum samples were collected for the immunoassay of tumor markers CEA and CA 19-9. Serum concentrations of CEA and CA 19-9 were measured using a commercial enzyme immunoassay kit (Abbott Co., Ltd., Tokyo, Japan). The cutoff values for serum CEA and CA 19-9 levels were 5.0 ng/ml and 37 U/ml, respectively [28].

Blood Processing and RNA Isolation

All blood specimens (5 ml) were preoperatively collected into tubes containing sodium citrate, and blood cells were separated using lymphocyte separation buffer (Gentra Systems, Inc., Minneapolis, Minn., USA). Total RNA was extracted from cell lines and blood specimens using Isogen (Nippon Gene, Toyama, Japan). Total RNA was isolated and purified using phenol-chloroform extraction, as described previously [25, 26]. The concentration and purity of total RNA were examined using a GeneQuant pro UV/Vis spectrophotometer (Amersham Pharmacia Biotech, Cambridge, UK).

Quantitative RT-PCR Analysis

Primer and probe sequences of STC 1 and glyceraldehyde-3-phosphatase dehydrogenase (GAPDH) were designed for quantitative RT-PCR (qRT-PCR) assay. The forward primers, fluorescence resonance energy transfer probe sequence, and reverse primers for STC 1 and GAPDH were as follows: STC 1 (forward), 5′-CACTTCTCCAACAGATACT-3′; (probe), 5′-FAM–CCTGCTGGAATGTGATGAAGACAC–TAMRA-1-3′; (reverse), 5′-CATGTTAGGCCCAATTTTC-3′; GAPDH (forward), 5′-GGGTGTGAACCATGAGAAGT-3′; (probe), 5′-FAM–CAGCAATGCCTCCTGCACCACCAA–TAMRA-1-3′, and (reverse), 5′-GACTGTGGTCATGAGTCCT-3′. The RT-PCR product sizes of STC 1 and GAPDH were 111 and 136 base pair fragments, respectively. The integrity of the RNA was assessed by RT-PCR assay using GAPDH.

All total RNA samples were reverse transcribed using the Advantage RT-for-PCR kit (Clontech Laboratories, Inc., Palo Alto, Calif., USA), as described previously [25, 26]. Samples were

analyzed by qRT-PCR assay using the LightCycler System (Roche Diagnostics, Mannheim, Germany). The reaction mixtures contained cDNA transcribed from 250 ng of RNA using each primer, probe, $MgCl_2$ and LightCycler FastStart DNA Master hybridization probes (Roche). The amplification profile comprised precycling at 95°C for 10 min followed by 40 cycles of denaturation at 95°C for 10 s, annealing for 20 s (60°C for STC 1 and 55°C for GAPDH) and extension at 72°C for 10 s. Plasmids for each marker were synthesized using pT7Blue-2 T-Vector (Novagen, Madison, Wisc., USA) according to the manufacturer's instructions. Standard curves for each assay were generated using the threshold cycles of six serial dilutions of plasmid templates (10^6–10^1 copies). The mRNA copy number was calculated using LightCycler software (Roche). Each assay was repeated in duplicate with positive (cancer cell line), negative (H_2O) and reagent (without cDNA) controls to confirm the validity of the qRT-PCR assay. Absolute copy numbers in qRT-PCR assay were determined on the basis of standard curves with six serial dilutions of plasmid templates. STC 1 mRNA copy numbers were normalized by GAPDH mRNA copy numbers (relative STC 1 mRNA copies; absolute STC 1 mRNA copies/absolute GAPDH mRNA copies).

IHC Analysis

The PEAT sections (3 μm thick) were incubated on slides at 50°C overnight, deparaffinized with xylene and then rehydrated with a graded series of ethanol. These sections were autoclaved in citrate buffer (0.01 mol/l, pH 6.0) at 120°C for 10 min to activate the antigen. Endogenous peroxidase was blocked using peroxidase blocking reagent (DakoCytomation, Carpinteria, Calif., USA) for 10 min after cooling at room temperature. Non-specific binding was blocked at room temperature for 30 min with a serum-free protein block (DakoCytomation). The sections were incubated at 4°C overnight with an anti-human STC 1 polyclonal antibody (Santa Cruz Biotechnology, Inc., Santa Cruz, Calif., USA) diluted 1:50 in Dako antibody diluent with background-reducing components (DakoCytomation). After washing in phosphate-buffered saline (PBS), the reaction for anti-human STC 1 polyclonal antibody was developed by the ABC method (Vectastain ABC kit; Vector Laboratories, Burlingame, Calif., USA) and visualized using diaminobenzidine tetrahydrochloride (DakoCytomation) [29]. PBS without primary antibody was used as a negative control under the same conditions.

Statistical Analysis

Differences in STC 1 mRNA expression between cancer cell lines and normal PBLs from healthy volunteers, and between PBLs from patients with gastric cancer and healthy volunteers, were assessed by the Wilcoxon rank sum test. Receiver operating characteristic (ROC) curves and the area under the curve (AUC) were used to evaluate the predictive ability of STC 1 mRNA expression for discriminating patients with gastric cancer from normal healthy volunteers. The relationship between STC 1 mRNA expression and categorical clinicopathological factors was statistically analyzed by χ^2 and Fisher's exact tests. All statistical calculations were carried out using SAS statistical software (SAS Institute Inc., Cary, N.C., USA). A value of $p < 0.05$ was considered statistically significant.

Table 1. Expression of blood markers in 93 patients with gastric cancer

Blood markers	Expression, n (%)	
	negative	positive
Serum CEA	68 (73.1)	25 (26.9)
Serum CA 19-9	70 (75.3)	23 (24.7)
STC 1	28 (30.1)	65 (69.9)

Results

RT-PCR Analysis of STC 1 mRNA Expression in Cell Lines and Clinical Blood Specimens

We initially assessed STC 1 mRNA expression in five gastric cancer cell lines and clinical blood specimens from 93 patients with gastric cancer and 21 healthy volunteers using qRT-PCR assay.

The relative numbers of STC 1 mRNA copies ranged from 3.15×10^{-5} to 2.97×10^{-3} in gastric cancer cell lines, from 0 to 8.39×10^{-4} in blood specimens of patients with gastric cancer, and from 0 to 2.14×10^{-6} in blood specimens of healthy volunteers. The mean relative numbers of STC 1 mRNA copies (±SD) were $8.47 \times 10^{-4} \pm 1.25 \times 10^{-3}$ in gastric cancer cell lines, $1.02 \times 10^{-5} \pm 8.69 \times 10^{-5}$ in blood specimens of patients with gastric cancer, and $3.44 \times 10^{-7} \pm 6.12 \times 10^{-7}$ in blood specimens of healthy volunteers (fig. 1). Finally, the relative numbers of STC 1 mRNA copies were significantly higher in gastric cancer cell lines and blood specimens of patients with gastric cancer than in blood specimens of healthy volunteers ($p = 0.0001$ and $p = 0.003$, respectively).

Comparison of the Clinical Utility between STC 1 and Conventional Serum Markers for Cancer Detection

ROC analysis statistically demonstrated that the AUC value for cancer detection based on the levels of STC 1 mRNA expression was 0.702 (fig. 2). The values of sensitivity and specificity of STC 1 mRNA were 0.699 and 0.714, respectively. Consequently, RT-PCR analysis demonstrated that 65 of 93 (69.9%) patients were positive for STC 1. On the other hand, positive rates of serum CEA and CA 19-9 in the same population were 26.9 (25/93) and 24.7% (23/93), respectively. Thus, the positive rate of STC 1 mRNA was higher than those of serum CEA and CA 19-9 (table 1).

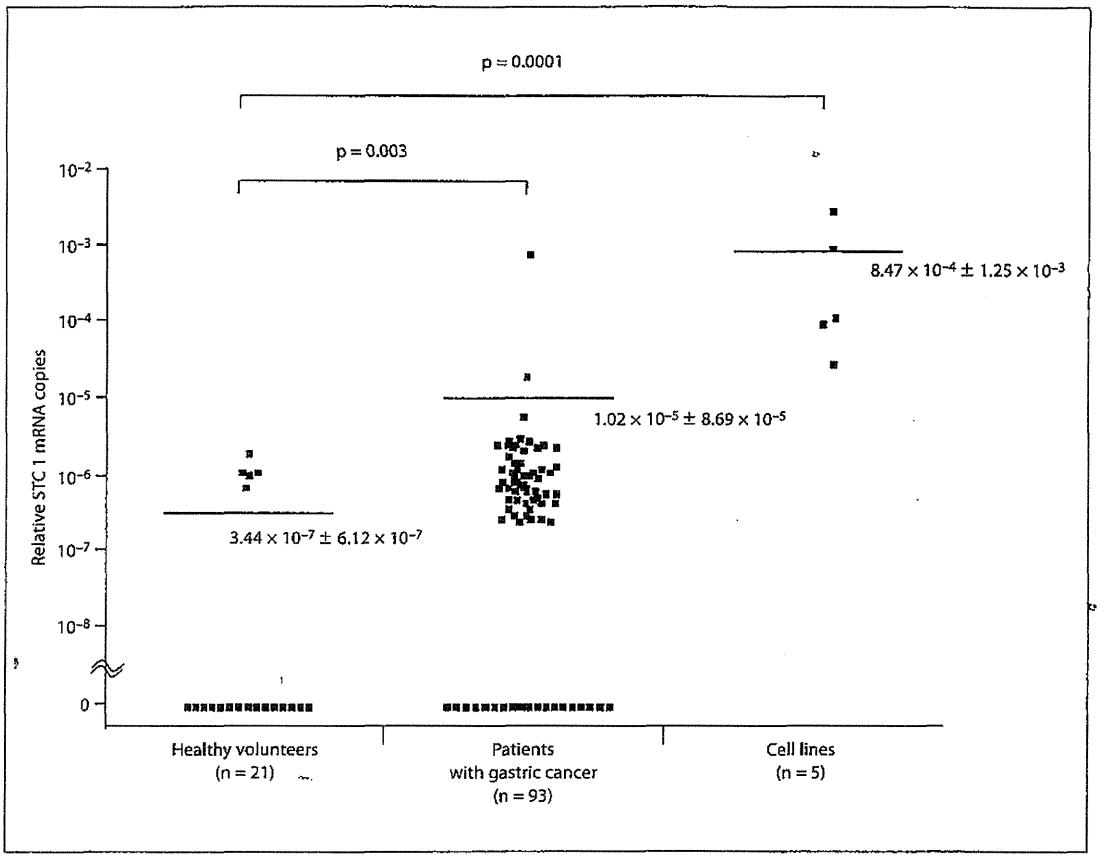

Fig. 1. RT-PCR analysis of STC 1 mRNA expression in cell lines and clinical blood specimens. Horizontal bars indicate mean number of STC 1 mRNA copies.

Correlation between STC 1 Expression and Clinicopathological Findings

To assess the relationship between the status of STC 1 expression and clinicopathological findings, all patients enrolled in this study were divided into two groups based on the presence or absence of STC 1 mRNA expression (positive, n = 65; negative, n = 28).

The status of STC 1 expression was significantly correlated with depth of tumor invasion and stage ($p = 0.032$ and $p = 0.013$, respectively; table 2).

IHC Analysis of STC 1 Protein Expression in Primary Tumor Specimens

To assess STC 1 expression in primary tumor cells, 20 surgical PEAT primary specimens obtained from patients with STC 1-positive expression in blood specimens were used for IHC analysis.

IHC analysis demonstrated STC 1 protein expression in the cytoplasm of tumor cells (fig. 3). Although immunoreactivity for STC 1 was variable in primary tumor cells, STC 1was expressed in all PEAT specimens (fig. 3).

Discussion

In the present study, we examined STC 1 mRNA expression by qRT-PCR assay in blood specimens from patients with gastric cancer and normal healthy volunteers. To assess the clinical utility of STC 1 as a diagnostic biomarker, we next compared the sensitivity of STC 1 with those of conventional serum markers, such as CEA and CA 19-9. Furthermore, we investigated the clinical impact of STC 1 expression in patients with gastric cancer. To our knowledge, this study is the first to demonstrate

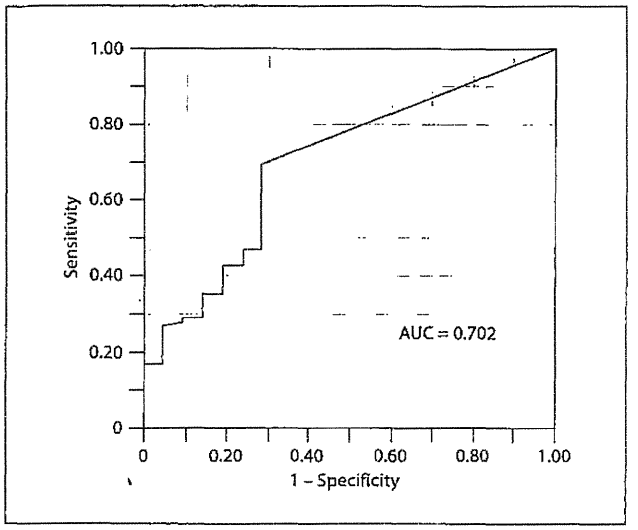

Fig. 2. ROC curve for discriminating patients with gastric cancer from healthy volunteers on the basis of STC 1 mRNA expression. AUC = 0.702.

Table 2. Correlation between STC 1 expression and clinicopathological findings in patients with gastric cancer

Factors	STC 1 expression, n (%)		p value
	negative (n = 28)	positive (n = 65)	
Gender			
Male	21 (75.0)	43 (66.1)	0.470
Female	7 (25.0)	22 (33.9)	
Age			
<70 years	13 (46.4)	32 (49.2)	0.825
>70 years	15 (53.6)	33 (50.8)	
Tumor location			
Upper	10 (35.7)	21 (32.3)	0.925
Middle	8 (28.6)	21 (32.3)	
Lower	10 (35.7)	23 (35.4)	
Histological type			
Differentiated	15 (53.6)	31 (47.7)	0.656
Undifferentiated	13 (46.4)	34 (52.3)	
Tumor size			
<50 mm	12 (42.9)	21 (32.3)	0.353
>50 mm	16 (57.1)	44 (67.7)	
Depth of tumor invasion			
pT_1–T_2	14 (50.0)	17 (26.1)	0.032
pT_3-T_4	14 (50.0)	48 (73.9)	
Lymph node metastasis			
Negative	15 (53.6)	22 (33.9)	0.106
Positive	13 (46.4)	43 (66.1)	
Stage			
I	14 (50.0)	14 (21.5)	0.013
II–IV	14 (50.0)	51 (78.5)	
Lymphatic invasion			
Negative	13 (46.4)	17 (26.1)	0.089
Positive	15 (53.6)	48 (73.9)	
Venous invasion			
Negative	13 (46.4)	18 (27.7)	0.096
Positive	15 (53.6)	47 (72.3)	

Except for tumor location (χ^2 test), p values were examined by Fisher's exact test. pT_1 = Invasion of lamina propria or submucosa; pT_2 = invasion of muscularis propria; pT_3 = invasion of subserosa; pT_4 = penetration of serosa without invasion of adjacent structures or invasion of adjacent structures.

STC 1 expression in blood specimens from patients with gastric cancer.

Initially, we verified a high level of STC 1 mRNA expression in all gastric cancer cell lines. We next demonstrated high STC 1 expression in blood specimens from patients with gastric cancer, in comparison with those from normal healthy volunteers. Moreover, the sensitivity of STC 1 mRNA was higher than those of serum CEA and CA 19-9 in terms of diagnostic efficacy. Similarly, Du et al. [24] reported that the level of STC 1 mRNA in blood specimens from patients with non-small cell lung cancer was significantly higher than in blood specimens from patients with benign pulmonary disease. Consequently, they concluded that STC 1 is a potential biomarker for patients with non-small cell lung cancer [24]. These results suggest that STC 1 is one of the candidate blood markers for monitoring CTC in patients with selected cancers, including gastric cancer. Currently, chemotherapy is widely performed in patients with unresectable advanced or recurrent gastric cancer. However, it is difficult to assess its effect precisely using conventional examinations such as a blood test for serum CEA and CA 19-9, gastrointestinal fiberscopy, double-contrast gastrography and computed tomography. Matsusaka et al. [30] reported that the monitoring assay of CTC is a useful tool for the assessment of the response to chemotherapy in patients with advanced gastric cancer. Further studies will be needed to verify the clinical efficacy of the STC 1-targeting qRT-PCR assay for predicting chemotherapeutic effects in patients with unresectable advanced or recurrent gastric cancer.

In the present study, we demonstrated that the presence of STC 1 expression was significantly correlated with tumor aggressiveness, such as depth of tumor invasion and stage. The 5-year survival rates of our patients with STC 1-positive and -negative expression were 64.4 and

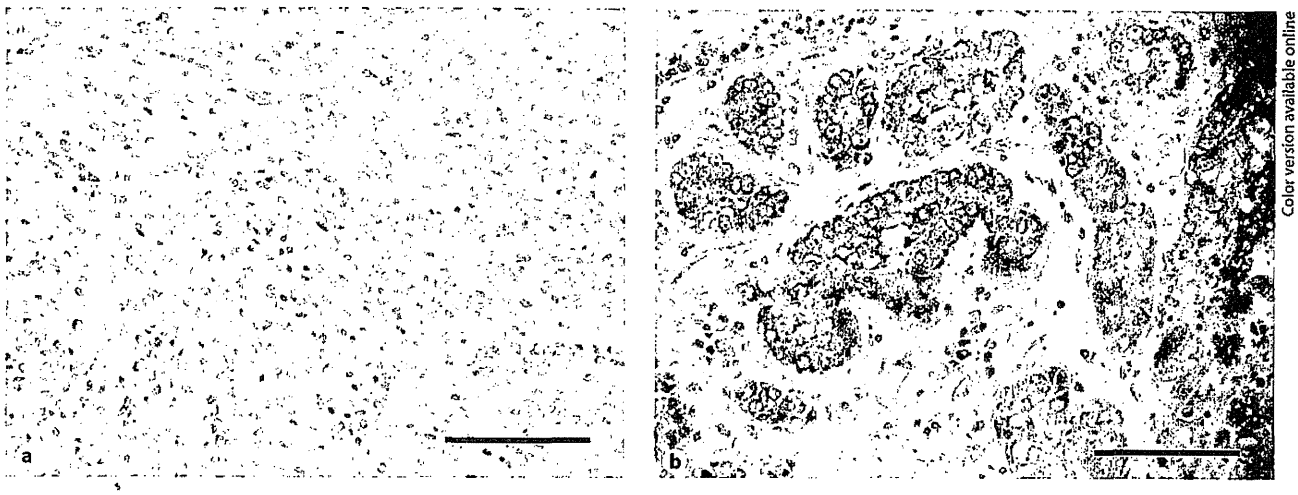

Fig. 3. Representative IHC of STC 1 protein expression in primary gastric tumor specimens. **a** Tumor cells with weak expression of STC 1. **b** Tumor cells with strong expression of STC 1. Scale bars = 100 μm (original magnification ×400).

79.4%, respectively. However, none of these differences reached statistical significance (data not shown). There are some possible explanations for this result: (a) The follow-up period was short (median, 25 months); (b) Patients receiving postoperative chemotherapy were included in this study and the selection criteria for postoperative chemotherapy were ambiguous in terms of the historical background. (c) The sample size may be too small for the identification of valid differences. Although further large studies are required to validate our results, the assessment of STC 1 expression in peripheral blood specimens might allow the preoperative prediction of aggressive disease behavior that has substantial influence on the therapeutic management of patients with gastric cancer.

To date, the biological role of STC 1 expression in tumor cells has not been sufficiently elucidated. However, Liu et al. [17] reported that the anti-apoptotic effect of STC 1 was inhibited by neutralizing anti-STC 1 monoclonal antibodies in in vitro assays. Furthermore, He et al. [18] reported that STC 1 promoted expression of VEGF related to angiogenesis via the activation of PKCβ II and ERK 1/2 pathways in in vitro assays. In this study, we confirmed STC 1 expression in blood specimens from patients with gastric cancer. Therefore, in the near future, it is necessary to elucidate the detailed mechanism of the STC 1 signaling pathway in gastric cancer.

In conclusion, we demonstrated that STC 1 is expressed in CTC and that its expression is closely correlated with tumor progression. Further studies on its biological role might lead to a novel molecular therapy that suppresses the STC 1 signaling pathway in patients with gastric cancer.

Acknowledgment

We thank Ms. A. Harada for technical assistance. This work was supported in part by a grant-in-aid (No. 22791256) for scientific research from the Ministry of Education, Science, Sports, and Culture of Japan.

Disclosure Statement

The authors have no conflicts of interest.

References

1 Statistics and Information Department, Ministry of Health, Labor, and Welfare: Vital Statistics of Japan 2004. Tokyo, Health and Welfare Statistics Association, 2006.
2 Ohtsu A: Current status and future prospects of chemotherapy for metastatic gastric cancer: a review. Gastric Cancer 2005;8:95–102.
3 Sakuramoto S, Sasako M, Yamaguchi T, Kinoshita T, Fujii M, Nashimoto A, Furukawa H, Nakajima T, Ohashi Y, Imamura H, Higashino M, Yamamura Y, Kurita A, Arai K, ACTS-GC Group: Adjuvant chemotherapy for gastric cancer with S-1, an oral fluoropyrimidine. N Engl J Med 2007;357:1810–1820.

4 Koizumi W, Narahara H, Hara T, Takagane A, Akiya T, Takagi M, Miyashita K, Nishizaki T, Kobayashi O, Takiyama W, Toh Y, Nagaie T, Takagi S, Yamamura Y, Yanaoka K, Orita H, Takeuchi M: S-1 plus cisplatin versus S-1 alone for first-line treatment of advanced gastric cancer (SPIRITS trial): a phase III trial. Lancet Oncol 2008;9:215–221.
5 Bang YJ, Van Cutsem E, Feyereislova A, Chung HC, Shen L, Sawaki A, Lordick F, Ohtsu A, Omuro Y, Satoh T, Aprile G, Kulikov E, Hill J, Lehle M, Rüschoff J, Kang YK, ToGA Trial Investigators: Trastuzumab in combination with chemotherapy versus chemotherapy alone for treatment of HER2-positive advanced gastric or gastro-oesophageal junction cancer (ToGA): a phase 3, open-label, randomised controlled trial. Lancet 2010;376:687–697.
6 Cristofanilli M, Budd GT, Ellis MJ, Stopeck A, Matera J, Miller MC, Reuben JM, Doyle GV, Allard WJ, Terstappen LW, Hayes DF: Circulating tumor cells, disease progression, and survival in metastatic breast cancer. N Engl J Med 2004;351:781–791.
7 Cohen SJ, Punt CJ, Iannotti N, Saidman BH, Sabbath KD, Gabrail NY, Picus J, Morse M, Mitchell E, Miller MC, Doyle GV, Tissing H, Terstappen LW, Meropol NJ: Relationship of circulating tumor cells to tumor response, progression-free survival, and overall survival in patients with metastatic colorectal cancer. J Clin Oncol 2008;26:3213–3221.
8 Hiraiwa K, Takeuchi H, Hasegawa H, Saikawa Y, Suda K, Ando T, Kumagai K, Irino T, Yoshikawa T, Matsuda S, Kitajima M, Kitagawa Y: Clinical significance of circulating tumor cells in blood from patients with gastrointestinal cancers. Ann Surg Oncol 2008;15:3092–3100.
9 Krebs MG, Sloane R, Priest L, Lancashire L, Hou JM, Greystoke A, Ward TH, Ferraldeschi R, Hughes A, Clack G, Ranson M, Dive C, Blackhall FH: Evaluation and prognostic significance of circulating tumor cells in patients with non-small-cell lung cancer. J Clin Oncol 2011;29:1556–1563.
10 Chang AC, Janosi J, Hulsbeek M, de Jong D, Jeffrey KJ, Noble JR, Reddel RR: A novel human cDNA highly homologous to the fish hormone stanniocalcin. Mol Cell Endocrinol 1995;112:241–247.
11 Olsen HS, Cepeda MA, Zhang QQ, Rosen CA, Vozzolo BL: Human stanniocalcin: a possible hormonal regulator of mineral metabolism. Proc Natl Acad Sci USA 1996;93:1792–1796.
12 Wagner GF, Jaworski EM, Haddad M: Stanniocalcin in the seawater salmon: structure, function, and regulation. Am J Physiol 1998;274:1177–1185.
13 Chang AC, Reddel RR: Identification of a second stanniocalcin cDNA in mouse and human: stanniocalcin 2. Mol Cell Endocrinol 1998;141:95–99.
14 Ishibashi K, Imai M: Prospect of a stanniocalcin endocrine/paracrine system in mammals. Am J Physiol Renal Physiol 2002;282:367–375.
15 Chang AC, Jellinek DA, Reddel RR: Mammalian stanniocalcins and cancer. Endocr Relat Cancer 2003;10:359–373.
16 Yeung HY, Lai KP, Chan HY, Mak NK, Wagner GF, Wong CK: Hypoxia-inducible factor-1-mediated activation of stanniocalcin-1 in human cancer cells. Endocrinology 2005;146:4951–4960.
17 Liu G, Yang G, Chang B, Mercado-Uribe I, Huang M, Zheng J, Bast RC, Lin SH, Liu J: Stanniocalcin 1 and ovarian tumorigenesis. J Natl Cancer Inst 2010;102:812–827.
18 He LF, Wang TT, Gao QY, Zhao GF, Huang YH, Yu LK, Hou YY: Stanniocalcin-1 promotes tumor angiogenesis through up-regulation of VEGF in gastric cancer cells. J Biomed Sci 2011;18:39.
19 Shirakawa M, Fujiwara Y, Sugita Y, Moon JH, Takiguchi S, Nakajima K, Miyata H, Yamasaki M, Mori M, Doki Y: Assessment of stanniocalcin-1 as a prognostic marker in human esophageal squamous cell carcinoma. Oncol Rep 2012;27:940–946.
20 Yeung BH, Law AY, Wong CK: Evolution and roles of stanniocalcin. Mol Cell Endocrinol 2012;349:272–280.
21 Wascher RA, Huynh KT, Giuliano AE, Hansen NM, Singer FR, Elashoff D, Hoon DS: Stanniocalcin-1: a novel molecular blood and bone marrow marker for human breast cancer. Clin Cancer Res 2003;9:1427–1435.
22 Nakagawa T, Martinez SR, Goto Y, Koyanagi K, Kitago M, Shingai T, Elashoff DA, Ye X, Singer FR, Giuliano AE, Hoon DS: Detection of circulating tumor cells in early-stage breast cancer metastasis to axillary lymph nodes. Clin Cancer Res 2007;13:4105–4110.
23 Tamura S, Oshima T, Yoshihara K, Kanazawa A, Yamada T, Inagaki D, Sato T, Yamamoto N, Shiozawa M, Morinaga S, Akaike M, Kunisaki C, Tanaka K, Masuda M, Imada T: Clinical significance of STC1 gene expression in patients with colorectal cancer. Anticancer Res 2011;31:325–329.
24 Du YZ, Gu XH, Li L, Gao F: The diagnostic value of circulating stanniocalcin-1 mRNA in non-small cell lung cancer. J Surg Oncol 2011;104:836–840.
25 Arigami T, Natsugoe S, Uenosono Y, Arima H, Mataki Y, Ehi K, Yanagida S, Ishigami S, Hokita S, Aikou T: Lymphatic invasion using D2–40 monoclonal antibody and its relationship to lymph node micrometastasis in pN0 gastric cancer. Br J Cancer 2005;93:688–693.
26 Arigami T, Natsugoe S, Uenosono Y, Mataki Y, Ehi K, Higashi H, Arima H, Yanagida S, Ishigami S, Hokita S, Aikou T: Evaluation of sentinel node concept in gastric cancer based on lymph node micrometastasis determined by reverse transcription-polymerase chain reaction. Ann Surg 2006;243:341–347.
27 Edge SB, Byrd DR, Compton CC, Fritz AG, Greene FL, Trotti A (eds): AJCC Cancer Staging Manual, ed 7. New York, Springer, 2010.
28 Oue N, Sentani K, Noguchi T, Ohara S, Sakamoto N, Hayashi T, Anami K, Motoshita J, Ito M, Tanaka S, Yoshida K, Yasui W: Serum olfactomedin 4 (GW112, hGC-1) in combination with Reg IV is a highly sensitive biomarker for gastric cancer patients. Int J Cancer 2009;125:2383–2392.
29 Hsu SM, Raine L, Fanger H: Use of avidin-biotin-peroxidase complex (ABC) in immunoperoxidase techniques: a comparison between ABC and unlabeled antibody (PAP) procedures. J Histochem Cytochem 1981;29:577–580.
30 Matsusaka S, Chin K, Ogura M, Suenaga M, Shinozaki E, Mishima Y, Terui Y, Mizunuma N, Hatake K: Circulating tumor cells as a surrogate marker for determining response to chemotherapy in patients with advanced gastric cancer. Cancer Sci 2010;101:1067–1071.

Cancer Science
The official journal of the Japanese Cancer Association JCA

Interferon-alpha modulates the chemosensitivity of CD133-expressing pancreatic cancer cells to gemcitabine

Tomomi Hayashi,[1,2,4] Qiang Ding,[1,4] Taisaku Kuwahata,[1,2] Koki Maeda,[1,2] Yumi Miyazaki,[1] Shuichiro Matsubara,[1] Toru Obara,[1] Shoji Natsugoe[2] and Sonshin Takao[1,3]

[1]Cancer and Regenerative Medicine, Frontier Science Research Center, Kagoshima University Graduate School of Medical and Dental Sciences, Kagoshima; [2]Department of Digestive Surgery, Kagoshima University Graduate School of Medical and Dental Sciences, Kagoshima, Japan

(Received October 25, 2011/Revised January 19, 2012/Accepted January 30, 2012/Accepted manuscript online February 9, 2012/Article first published online March 13, 2012)

Pancreatic cancer is a lethal disease as current chemotherapies with gemcitabine (GEM) are still insufficient. Accumulating evidence suggests that cancer stem cells (CSC) are responsible for chemoresistance and that CD133 is one of the CSC markers in pancreatic cancer. Interferon-alpha (IFN-α), a cytokine with pleiotropic effects, has direct cytotoxic and cytostatic effects on tumor cells. The aim of the present study was to investigate whether IFN-α can modulate the chemosensitivity of a human pancreatic cancer cell line, Capan-1, to GEM. Cell cycles were evaluated for response to GEM with and without IFN-α by BrdU assay. GEM inhibited Capan-1 cell growth in a dose-dependent manner. GEM (IC_{50}; 100 ng/mL) treatment reduced the number of both $CD133^+$ and $CD133^-$ cells in the S phase, induced apoptosis of $CD133^-$ cells more than that of $CD133^+$ cells and increased accumulation of $CD133^+$ cells into the G0/G1 phase. These results infer that $CD133^+$ cells take shelter into the G0/G1 phase from GEM treatment. IFN-α modulated $CD133^+$ cells from the G0/G1 phase to the S phase. Consequently, apoptosis was accelerated in both $CD133^+$ and $CD133^-$ cells after IFN-α combined with GEM treatment. Furthermore, GEM combined with IFN-α treatment showed a significant tumor suppressive effect in the *in vivo* study. Importantly, $CD133^+$ cells showed CSC-like properties, such as generation of spheres, highly invasive ability and high tumorigenesis. These results suggest that IFN-α, as a modulator, could contribute to the treatment of $CD133^+$ cancer cells and be effective in combined chemotherapies with GEM for pancreatic cancer stem-like cells. (*Cancer Sci* 2012; 103: 889–896)

Pancreatic cancer is a lethal disease with a 5-year survival rate of 5%,[1] and recurs despite the use of current chemotherapies. Over the past decade, accumulating evidence has led to the development of the cancer stem cell (CSC) hypothesis for solid tumors.[2,3] This hypothesis might explain the poor prognosis of pancreatic cancer patients because a few CSC can sustain tumor growth and drive relapse after curative treatments. Importantly, CSC contribute to drug resistance.[4,5]

CD133 has been implicated as a CSC marker in some cancers.[6–14] In contrast, whether CD133 is a marker of CSC or progenitor cells has been a matter of debate.[15,16] We previously reported that CD133 expression is an unfavorable factor for survival of pancreatic cancer patients.[17] Furthermore, CD133-expressing CSC are essential for the development and perpetuation of pancreatic cancer,[18] and may account for resistance to current and standard chemotherapy drugs, such as gemcitabine (GEM).[19] However, whether CD133 expression is involved in anti-cancer drug resistance is unknown.

Interferon-alpha (IFN-α), a cytokine with pleiotropic effects, possesses direct cytotoxic and cytostatic effects on tumor cells as well as antiangiogenic effects, and also activates antitumor immunity.[20–23] IFN-α attracted our interest because of its contribution to the reduction of the side population (SP) enriched in stem cells,[24] which was defined by the poor accumulation of Hoechst 33342 in ovarian cancer cells.[25] Experimentally, IFN-α at the optimal biological dose schedule, and in combination with GEM, has been shown to induce apoptosis in tumor-associated endothelial cells and to decrease the growth of human pancreatic cancer cells.[26] However, effects of IFN-α on CSC in pancreatic cancer have not yet been validated.

Here, we investigate the chemosensitivity of pancreatic cancer cells in the presence of CD133 expression and whether IFN-α can modulate GEM resistance.

Materials and Methods

Cell culture and reagents. A human pancreatic cancer cell line, Capan-1, was obtained from the American Type Culture Collection (Manassas, VO, USA). Cells were cultured in DMEM/F12 medium (Gibco, Carlsbad, CA, USA) containing 10% FBS, 100 U/mL penicillin and 100 mg/mL streptomycin at 37°C in 5% CO_2. GEM was supplied by Eli Lilly Japan (Tokyo, Japan), and recombinant human IFN-α was purchased from Acris Antibodies GmbH (Herford, Germany). GEM and IFN-α were diluted in culture medium immediately before use.

Flow cytometric analysis and fluorescence-activated cell sorting. In the present study, 10^6 single cells were suspended into 100 μL PBS containing 0.5% BSA. A total of 20 μL of FcR blocking reagent and antibodies, carboxyfluorescein conjugated mouse anti-human IFN-α/β receptor 1 (R&D Systems, Minneapolis, MN, USA) or R-phycoerythrin (PE)-conjugated mouse monoclonal anti-human IFN-α/β receptor 2 (PBL Interferon-Source, Piscataway, NJ, USA) were added at the appropriate dilutions and incubated on ice for 10–20 min in the dark. Cells were washed and resuspended in a suitable amount of buffer for analysis by flow cytometry. Flow cytometric analysis and FACS were carried out with a FACSAria (Becton Dickinson, Franklin Lakes, NJ, USA) and FACSDiva (BD Biosciences, San Jose, CA, USA). Dead cells were excluded by 7-amino-actinomycin-D (7-AAD; BD Pharmingen, San Diego, CA, USA) staining. Anti-CD133-PE (Miltenyi Biotec, Cologne, Germany) were used for sorting $CD133^+$ and $CD133^-$ subpopulations of Capan-1 cells. FACSAria sorting routinely achieved purities exceeding 95% in cell fractions.

Sphere forming assay. Spheres were cultured in DMEM/F12 serum-free medium supplemented with epidermal growth

[3]To whom correspondence should be addressed.
E-mail: sonshin@m2.kufm.kagoshima-u.ac.jp
[4]These authors contributed equally to this work.

doi: 10.1111/j.1349-7006.2012.02235.x

factor (20 ng/mL; Cell Signaling Tech, Danvers, MA, USA), basic fibroblast growth factor (10 ng/mL; PeproTech, London, UK) and B27 supplements (1:50; Gibco). Capan-1 cells were cultured for 7 days. Immunofluorescence staining was performed on spheres in culture to identify CD133 expression. Cells were fixed with 10% formalin prior to immunostaining, then incubated with anti-CD133 mAb for 2 h at 37°C and subsequently washed three times with PBS containing 2% FBS. Next, the cells were incubated for 1 h with PE-conjugated anti-mouse secondary antibodies. Nuclear was stained by DAPI. Finally, the stained cells were viewed under a confocal laser scanning microscope (Olympus, Tokyo, Japan). The negative control groups contained cells stained only with the secondary antibody.

Migration and invasion assays. In total, 5×10^4 cells were seeded in serum-free medium into 24-well Falcon migration inserts (8 μm pore size). Inserts were placed in Falcon companion plates containing 10% FBS and incubated for 18 h for migration. For invasion, 5×10^4 cells were seeded in serum-free medium into a Matrigel invasion chamber (Becton Dickinson) for 22 h. Following incubation, the medium and cells were removed from the top chamber using cotton swabs and PBS. The number of migrating or invading cells on the underside of the membrane was determined by staining using Giemsa for 5 min. The number of migrating or invading cells in 10 fields was counted at 20× magnification using light microscopy.

Cytotoxicity assays. Capan-1 cells were resuspended in fresh medium at a concentration of 5×10^3 cells/100 μL and seeded in a 96-well plate, and cells were incubated for 48 h at 37°C. Then, GEM was added to each well at concentrations of 1, 5, 10, 50, 100, 500 and 1000 ng/mL to test the GEM treatment, or IFN-α was added to each well at concentrations of 500, 1000, 2500, 5000, 10 000, 25 000, 50 000 and 100 000 U/mL to test the IFN-α treatment. The plate was incubated at 37°C for another 48 h. For the assay, 10 μL of 3-(4,5-dimethylthiazol-2-yl)-2,5-diphenyltetrazolium bromide (MTT; 5 mg/mL) was added to each well, and the plate was incubated for an additional 3 h at 37°C. The medium and MTT solution were then aspirated, and 70 μL of DMSO (Sigma-Aldrich, St. Louis, MO, USA) was added. The absorbance was measured at 570 nm using a microplate reader.

BrdU assay. Cells (80–90% confluent) were incubated with 1 mM BrdU for 3 h at 37°C and processed using the fluorescein isothiocyanate BrdU Flow Kit (BD Biosciences) according to the manufacturer's instructions. Briefly, 1×10^6 trypsinized cells were fixed, permeabilized and digested with DNase. Cells were then stained with fluorescein isothiocyanate –conjugated anti-BrdU and 7-AAD. For cell isolation and characterization, anti-CD133/1-APC (Miltenyi Biotec) was used. For each experiment, 10^4 events were counted by flow cytometry and assays were performed in triplicate. Data were analyzed using FACSDiva.

Western blotting. Cells were lysed on ice in lysis buffer and the lysates were boiled for 5 min, clarified by centrifugation at 15 000*g* for 15 min, and then separated by SDS-PAGE. The proteins were transferred onto nitrocellulose membranes. The membranes were then incubated with a 1:200 dilution of

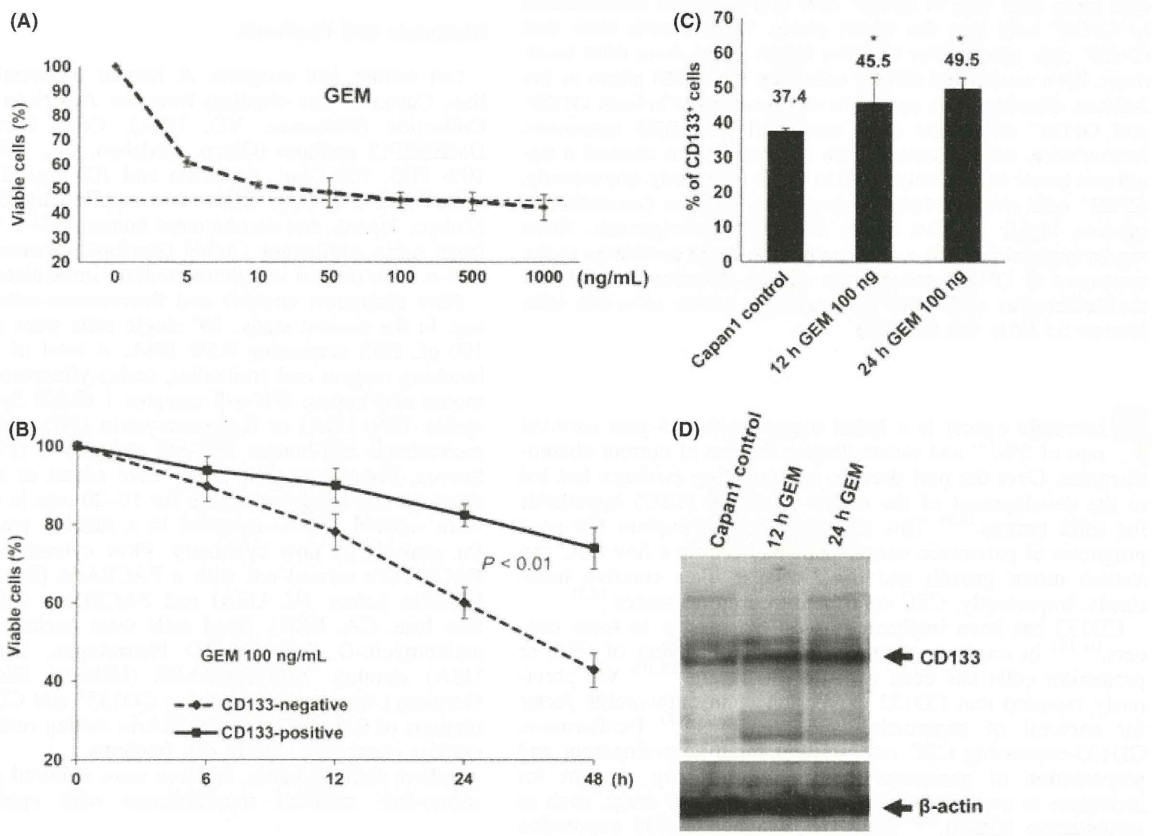

Fig. 1. CD133$^+$ Capan-1 cells are more resistant to gemcitabine (GEM) treatment than CD133$^-$ cells. (A) GEM inhibited Capan-1 cell growth in a dose-dependent manner, and its IC_{50} was 100 ng/mL. It was measured using the MTT growth inhibitory assay after 24 h of continuous GEM exposure. (B) GEM treatment (100 ng/mL) showed different sensitivities in CD133$^+$ and CD133$^-$ cells. Error bars indicate SD. (C) GEM treatment for 12 or 24 h increased the proportion of CD133$^+$ cells. Error bars indicate SD. *$P < 0.01$ *vs* control. (D) Western blot of CD133 expression.

doi: 10.1111/j.1349-7006.2012.02235.x

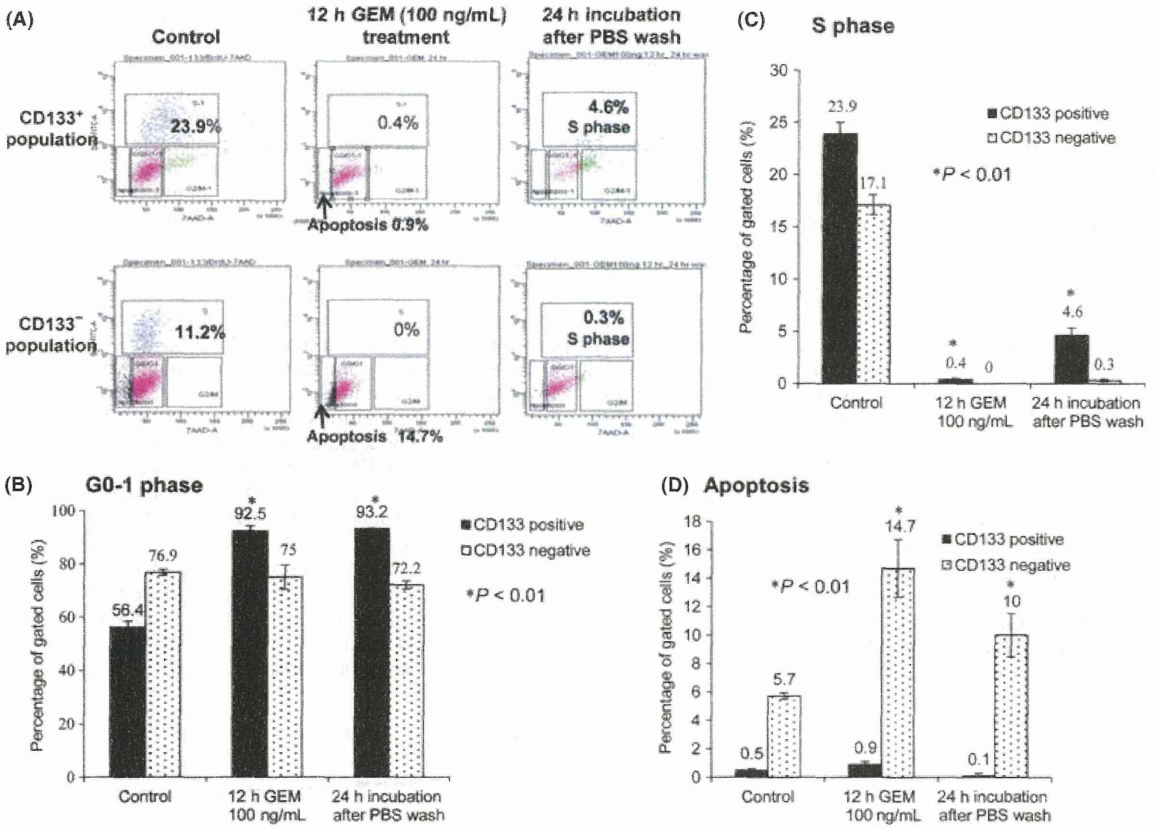

Fig. 2. Comparison of cell cycles between CD133$^+$ and CD133$^-$ cells. (A) Flow cytometry was used for cell cycle analysis before and after exposure to gemcitabine (GEM). Baseline data are provided in the left panel. Cells were then treated with GEM for 12 h (middle) followed by 24 h of recovery after withdrawal of GEM (right). (B) Comparison of CD133$^+$ and CD133$^-$ cells in the G0/G1 phase. (C) The S phase and (D) apoptosis by BrdU assay after GEM treatment. Results are based on three independent experiments. Error bars indicate SD. *P < 0.01 *vs* control.

anti-CD133 mAb (Miltenyi Biotec) followed by a 1:200–1000 dilution of peroxidase-conjugated anti-mouse IgG (Jackson ImmunoResearch, West Grove, PA, USA) antibody for the secondary reaction. As an internal control for the amount of protein loaded, β-actin was detected. The immunocomplex was visualized using the ECL western blot detection system (GE Healthcare Life Science, Amersham, UK).

Mitogen-activated protein kinase-integrating kinase 1 inhibition experiments. Capan-1 cells were pretreated with 20 μM CGP57380 (mitogen-activated protein kinase-integrating kinase [Mnk1] inhibitor; Sigma-Aldrich) for 60 min, and subsequently cultured with 10 μM CGP57380 during the treatment with IFN-α. Proteins were then detected with antibodies against the phosphorylated Mnk1 (Thr-197/202, 1:250 dilution; Cell Signaling Tech) and Mnk1 (1:250 dilution); 10% FCS treated cells were used as a positive control for Mnk1 phosphorylation. The signals for pMnk1 were quantified by densitometry using Image J software. To assess the effects of Mnk inhibition on cell viability, Capan-1 cells were treated with IFN-α, gemcitabine or Mnk1 inhibitor CGP57380 combination. After 48 h incubation, cell viability was determined by MTT assay.

Animal studies. The animal study was approved by the Committee on the Use of Live Animals for Teaching and Research of Kagoshima University. Non-obese diabetic (NOD)/SCID and BALB/c nu/nu (nude) mice were purchased from CLEA Japan (Tokyo, Japan).

Tumorigenic assay. For the tumorigenic assay, CD133$^+$ or CD133$^-$ populations of Capan-1 cells were collected using FACSAria and PE-conjugated anti-CD133 antibody. Freshly isolated CD133$^+$ and CD133$^-$ cells were subjected to tumorigenic assay. In total, 10, 100 and 1000 cells of each quadrant suspended in 50 μL of DMEM F-12 medium and 50 μL Matrigel were injected s.c. into 6-week-old NOD/SCID mice. Animals were maintained until death resulting from the neoplastic process or the end of the experiment. Xenograft tumors were fixed with 10% buffered formaldehyde and stained with H&E.

***In vivo* chemotherapies for xenograft tumors.** For *in vivo* treatments, nude mice were randomly assigned to four treatment groups of five mice at week 2 after s.c. injection of Capan-1 cells (5×10^5). Mice received treatments of vehicle (saline, i.p.), GEM (120 mg/kg/week, i.p.) alone, IFN-α (20 000 U/mouse/every 2 days, s.c.) alone, or GEM combined with IFN-α for 4 weeks. Growth curves of xenograft tumors in nude mice were assessed after treatments.

Statistical analysis. Group differences were analyzed statistically using the χ^2-test and Student's t-test. A P-value <0.05 was considered statistically significant. All statistical analyses were performed using StatView statistical software version 5.0 (SAS Institute, Cary, NC, USA).

Results

CD133$^+$ Capan-1 cells are resistant to gemcitabine treatment. CD133 expression was examined by flow cytometric analysis in several human pancreatic cancer cell lines. The positive ratio of CD133 in Capan-1cells is approximately 45%, higher than that in the other cell lines (Table S1), Capan-1 was chosen to evaluate the sensitivity to GEM. GEM inhibited

Capan-1 cell growth in a dose-dependent manner and its IC_{50}, as assessed by MTT growth inhibitory assay, was 100 ng/mL (Fig. 1A). The growth inhibition by GEM treatment (100 ng/mL) showed a significant ($P < 0.01$) difference between $CD133^+$ and $CD133^-$ populations of Capan-1 cells (Fig. 1B). GEM treatment increased the proportion of $CD133^+$ Capan-1 cells (Fig. 1C). Similarly, CD133 protein levels increased in a time-dependent manner (Fig. 1D). GEM treatment produced a significant increase in the G0/G1 phase and a decrease in the S phase cell populations (Fig. S1). We compared cell cycles between $CD133^+$ and $CD133^-$ populations of Capan-1 cells by BrdU assay after GEM treatment (Fig. 2A). The proportion of $CD133^+$ cells in the G0/G1 phase increased from 56.4 to 92.5%, and was maintained at 93.2% even after withdrawal of GEM (Fig. 2B). However, there were no significant changes in $CD133^+$ cells. Although the proportion of $CD133^+$ and $CD133^-$ cells in the S phase was remarkably reduced after GEM treatment, the proportion of $CD133^+$ cells in the S phase increased compared to that in $CD133^+$ cells after withdrawal of GEM (Fig. 2C). The proportion of $CD133^+$ cells in the apoptotic phase was significantly lower than that in $CD133^-$ cells under control, and apoptotic cells were highly induced in $CD133^+$ cells after GEM treatment and withdrawal of GEM (Fig. 2D). These results indicated that $CD133^+$ cells were resistant to GEM, compared to $CD133^-$ cells.

Interferon-alpha reduces the $CD133^+$ ratio of Capan-1 cells. All Capan-1 cells showed expression of IFN-α/β receptor 2 (Fig. 3A). IFN-α inhibited Capan-1 cell growth by up to 30% in a dose-dependent manner, and concentrations over 5000 U/mL showed similar inhibition rates (Fig. 3B). Importantly, IFN-α treatment decreased the proportion of $CD133^+$ cells in a time-dependent manner (Fig. S2, Fig. 3C). Similarly, after over 6 h of IFN-α treatment, CD133 protein levels were decreased (Fig. 3D). To understand the mechanism underlying IFN-α treatment, Mnk1 expression and inhibition experiment were performed. IFN-α treatment induced phosphorylation of Mnk1 in a time-dependent manner (Fig. 3E left and right). Mnk1 inhibitor CGP57380 administration antagonized the IFN-α effect on cell growth suppression, but not significantly. Mnk1 inhibitor mitigated the antiproliferative response to the co-administration of IFN-α and GEM (Fig. 3F).

Interferon-alpha contributes to combined chemotherapy with gemcitabine. We compared cell cycles between the $CD133^+$ and $CD133^-$ populations of Capan-1 cells by BrdU assay after GEM alone, IFN-α alone or GEM combined with IFN-α treatment (Fig. S3). GEM treatment increased the ratio of cells in the G0/G1 phase in the $CD133^+$ population, while IFN-α decreased the proportion of cells in the G0/G1 phase (Fig. 4A upper). In the $CD133^-$ cells, however, the G0/G1 phases were similar among these treatments (Fig. 4A lower). IFN-α, but not GEM treatment, remarkably increased the proportion of cells in the S phase in both $CD133^+$ and $CD133^-$ cells. Furthermore, GEM combined with IFN-α treatment significantly increased the apoptotic phases in both $CD133^+$ and $CD133^-$

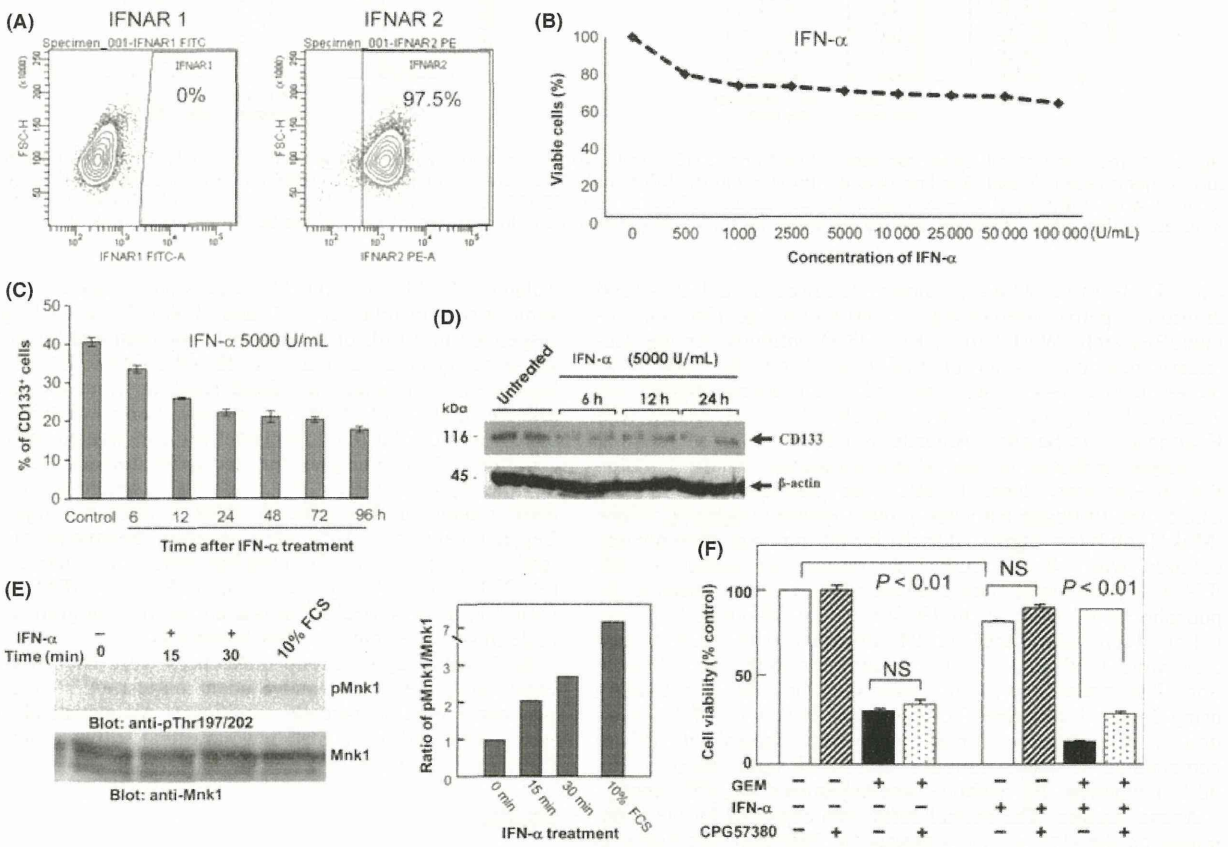

Fig. 3. Interferon-alpha (IFN-α) reduced the proportion of $CD133^+$ cells in Capan-1 cells. (A) Expressions of IFNAR 1 (left) and IFNAR 2 (right). (B) IFN-α inhibited Capan-1 cell growth in a dose-dependent manner for 48 h exposure. (C) IFN-α (5000 U/mL) treatment for 48 h decreased the proportion of $CD133^+$ cells in Capan-1 cells over time. (D) CD133 protein level analyzed by western blot. (E) IFN-α-dependent phosphorylation/activation of Mnk1 in a time-dependent manner (left and right). (F) Mnk1 mediated the antiproliferative response to the co-administration of IFN-α and gemcitabine (GEM). Capan-1 cells were treated in the combination of IFN-α, GEM and Mnk1 inhibitor CGP57380. After 48 h incubation, cell viability was determined by MTT assay. These results are the means and SD of values from four wells in one representative experiment.

doi: 10.1111/j.1349-7006.2012.02235.x

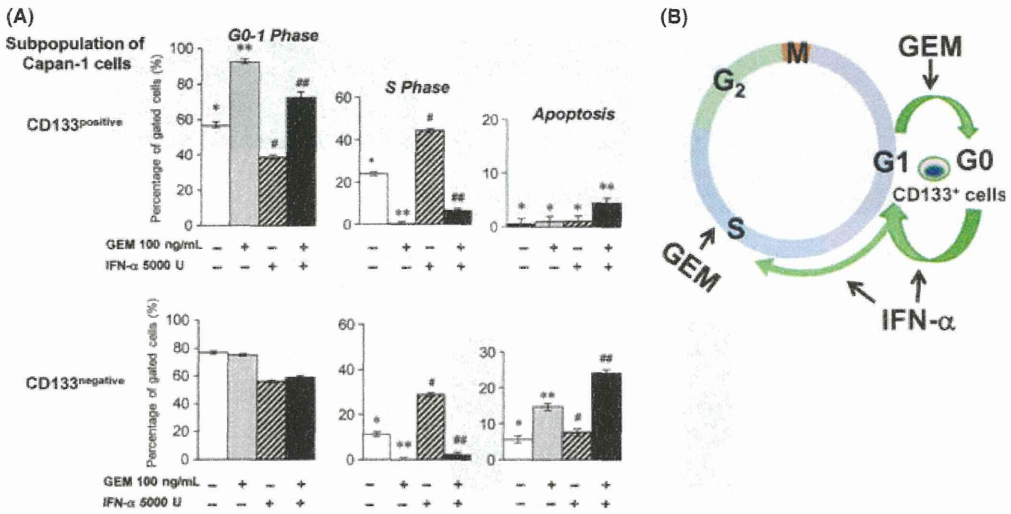

Fig. 4. Interferon-alpha (IFN-α) contributes to combined chemotherapy by reducing the proportion of the G0/G1 phase cells and increasing the proportion of the S phase and apoptotic cells. (A) Comparison of G0/G1, S and apoptotic cells by BrdU assay between $CD133^+$ and $CD133^-$ cells treated with gemcitabine (GEM) alone, IFN-α alone or GEM + IFN-α for 24 h. In $CD133^+$ (upper) and $CD133^-$ (lower) populations, * *vs* **, * *vs* # and # *vs* ## indicate $P < 0.01$. Error bars indicate SD. (B) Model of IFN-α modulating $CD133^+$ cells from G0/G1 to the S phase and targeting them combined with GEM.

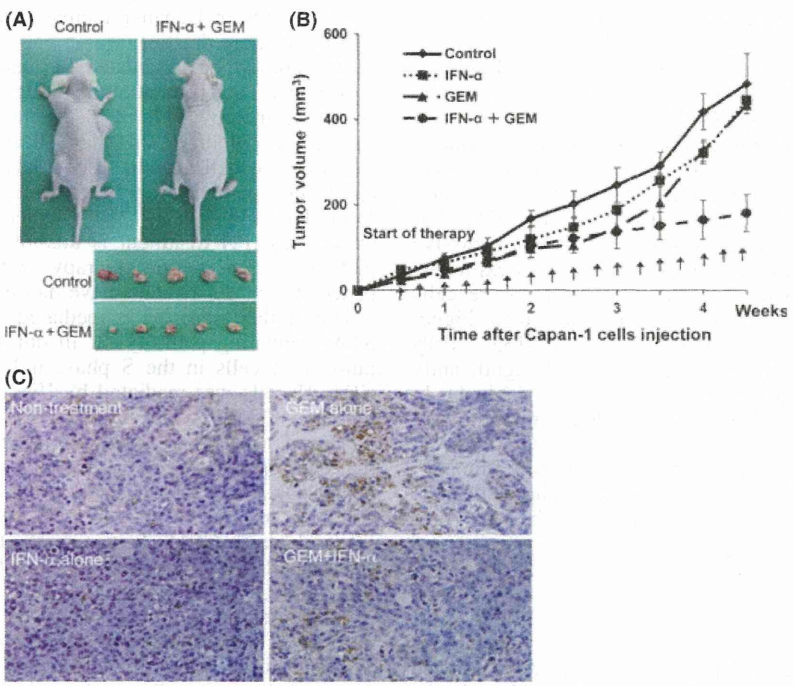

Fig. 5. *Effect of interferon-alpha (IFN-α) on the growth of xenograft Capan-1 tumor in nude mice.* (A) Xenograft tumors with IFN-α + gemcitabine (GEM) treatment were smaller than those with controls in nude mice. (B) Tumor growth curves of Capan-1 xenografts which were treated with GEM (100 ng/mL) alone, IFN-α (5000 U/mL) alone or GEM plus IFN-α. IFN-α + GEM treatment showed a significant effect ($P < 0.01$). (C) Comparison of histological CD133 expression in Capan-1 xenografts with treatments at week 5 after inoculation into nude mice.

cells (Fig. 4A). These results suggest that IFN-α modulates the cell cycle of $CD133^+$ Capan-1 cells (Fig. 4B).

Effect of interferon-alpha on xenograft tumors of $CD133^+$ cells. We attempted to determine the *in vivo* effect of IFN-α on xenograft tumors derived from Capan-1 cells in nude mice. Four weeks' treatment of GEM combined with IFN-α suppressed tumor growth in nude mice (Fig. 5A) and led to significant differences in tumor growth curves compared to the control, GEM alone or IFN-α alone (Fig. 5B). However, body weight did not change significantly (Fig. S4A). In the immunohistological study, xenograft tumor cells treated with GEM showed higher $CD133^+$ expression than those of the control. In

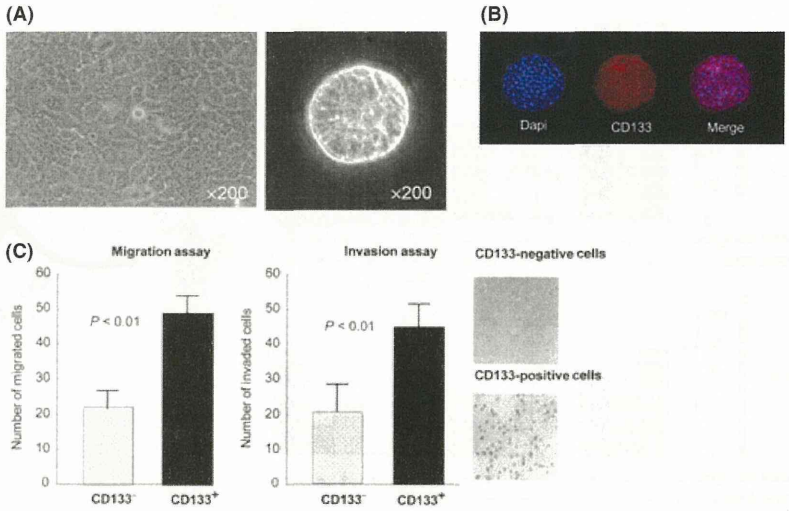

Fig. 6. Cancer stem-like characteristics were identified in CD133$^+$ Capan-1 cells. (A) Capan-1 cells showed monolayer growth in medium with serum (left). In serum-free culture, a sphere was generated after 10 days of culture (right). Magnification: ×200. (B) These sphere cells expressed CD133 by immunofluorescence staining. Magnification: ×200. (C) Comparison of migration and invasion abilities between CD133$^+$ and CD133$^-$ Capan-1 cells.

contrast, CD133$^+$ expression in xenograft tumors treated with IFN-α alone was lower than those with saline as control. Interestingly, xenograft tumors treated with GEM combined with IFN-α showed an intermediate CD133$^+$ expression (Fig. 5C). The flow cytometric analysis showed similar results to the immunohistological study (Fig. S4B).

CD133$^+$ Capan-1 cells identified as a cancer stem-like population of cells. Flow cytometric analysis was performed on several human pancreatic cancer cell lines. Among these, Capan-1 showed high expression of CD133 (Table S1, Fig. 6A). Capan-1 cells showed sphere formations in a stem cell-permissive medium without serum (Fig. S5A), and CD133 was expressed on the cell surface or in the cytoplasm in these sphere cells (Fig. 6B). These CD133$^+$ Capan-1 cells showed a higher potential of migration and invasion than CD133$^-$ cells (Fig. 6C). Furthermore, CD133$^+$ cells showed significantly greater tumorigenic potential than CD133$^-$ cells (Table 1). In these tumors, the histology was ductal adenocarcinoma and CK expression was observed in all tumor cells, while CD133 expression was shown in a part of the tumor cells by immunohistological staining (Fig. S5B). These results indicate that the CD133$^+$ population of Capan-1 cells exhibits CSC-like properties.

Discussion

Gemcitabine had greater inhibitory effects on the human pancreatic cancer cells, Capan-1. However, CD133$^+$ cells showed more resistance to GEM than CD133$^-$ cells, although the growth speed between CD133$^+$ and CD133$^-$ cells was the same in Capan-1. Along with GEM treatment, the ratio of CD133$^+$ cells in Capan-1 increased and the resistance against GEM was more drastic.

Interferon-alpha modulated the cell cycle, resulting in antiproliferative and proapoptotic effects on CD133$^+$ cells using combined therapy with GEM. Members of the IFN family are pleiotropic cytokines that have been shown to be important regulators of cell growth. IFN-α has been recognized to have therapeutic potential for the prevention and treatment of hepatocellular carcinoma.[27,28] Whether pancreatic cancer cells respond to IFN treatment is unknown, although clinical trials including combination therapy with IFN-α for advanced pancreatic cancer patients have had promising results.[29,30]

Type I IFN signaling is mediated by activation of the JAK-STAT signaling pathway.[31] In our study, the increase of the number of cells in the S phase indicates that proliferation of CD133$^+$ cells was mediated by IFN-α treatment. The accumulation of CD133$^+$ cells into the G0/G1 phase was remarkably increased after GEM treatment. GEM is a nucleoside analog that can replace one of the building blocks of the nucleic acid during DNA replication, leading to suppression tumor growth. Another target of GEM is to inactivate the enzyme ribonucleotide reductase. GEM shows specificity for proliferation in the S phase of the cell cycle with no effect on progress through early G1, G2 or M phases of the cell cycle.[32] However, IFN-α contributed to the effect on the decrease of CD133$^+$ cells in the G0/G1 phase and the increase of them in the S phase. IFN-α priming provides an efficient way to induce cell cycle entry of dormant cells, such as hematopoietic stem cells.[33] IFN-α makes dormant cells susceptible to elimination by antiproliferative chemotherapeutic drugs,[34] such as CD133$^+$ cells, as shown in Figure 4B. According to a recent report, the Mnk/eIF4E kinase pathway is activated in an IFN-inducible manner and plays important roles in mRNA translation for IFN-stimulated genes and in the generation of IFN-inducible antiproliferative responses.[35] In our study, IFN-α treatment induced rapid phosphorylation of Mnk1 that was detectable within 15 min of treatment. Mnk1 inhibitor may mitigate the antiproliferative response to the co-administration of IFN-α and GEM. Further clarification of tumor suppression by IFN-α is necessary.

Table 1. Comparison of tumorigenesis between CD133$^+$ and CD133$^-$ population cells in Capan-1 using non-obese diabetic/SCID mice

Subset of Capan-1	Number of implanted cells			Total
	10	10^2	10^3	
CD133$^+$	1/10 (10%)	7/10** (70%)	8/10** (80%)	16/30*** (53%)
CD133$^-$	0/10	0/10	1/10 (10%)	1/30 (3%)

***$P < 0.001$; **$P < 0.05$.

doi: 10.1111/j.1349-7006.2012.02235.x

Numerous studies have identified a "side population" (SP) in various tumor types,[36–39] and SP cells seem to be rich in stem cells.[24] These malignant SP cells proliferate in a sustained fashion and readily export many cytotoxic drugs. This high drug efflux capacity correlates with the strong expression of ATP-binding cassette transporters.[36] Interestingly, ovarian cancer containing SP cells have been found to be IFN-α sensitive *in vitro* and *in vivo* due to marked anti-proliferative and pro-apoptotic effects.[20] In this study, however, the $CD133^+$ population of Capan-1 cells did not coincide with the SP population (data not shown). IFN-α increased the number of $CD133^+$ cells in the S phase compared to that of $CD133^-$ cells. Furthermore, IFN-α combined with GEM induced apoptosis in both $CD133^+$ and $CD133^-$ cells to a greater extent than GEM or IFN-α treatment alone. IFN-α has also been shown to induce differentiation of lung cancer cells [37] and hepatic progenitors.[40] In addition, IFN-α has been shown to regulate the transition from SP into other phenotypes, although this IFN signaling-related mechanism is unclear.[25]

In our study, the combination of IFN-α and GEM significantly inhibited the growth of xenografts of Capan-1 cells compared to the control, GEM or IFN-α alone. These results were consistent with the *in vitro* data. However, using *in vivo* orthotopic pancreas cancer models, the combination of IFN-α and GEM has been reported to synergistically induce endothelial cell apoptosis.[26] These results suggest that IFN-α may have multiple biological functions in the modulation of gene expression and regulation of the cell cycle in terms of tumor suppression *in vivo*.

In contrast, $CD133^+$ population of Capan-1 cells exhibited greater tumorigenesis and the potential to generate spheres and aggressive behavior, such as migration and invasion, compared with $CD133^-$ cells. These results suggest that CD133 plays an important role in the cancer stem-like population of Capan-1 cells. Hence, the underlying mechanism of the CSC regulation is an important issue. In a recent study, the combined blockade of sonic hedgehog and mTOR signaling together with GEM treatment led to a profound depletion of the CSC compartment and shrinkage of established tumors.[41] Our results shed new light on the impact of IFN-α on the cell cycle of a CSC-like population in pancreatic cancer cells, although further research into the mechanism of the CSC modulation by IFN-α is still needed.

In the present study, we demonstrated that GEM could efficiently act on S phase cells in both $CD133^+$ and $CD133^-$. $CD133^+$ cells could escape from GEM treatment by retention in the G0/G1 phase. IFN-α administration prompted G0/G1 phase $CD133^+$ cells to re-enter the cell cycle. Thus, IFN-α treatment could increase GEM therapeutic efficacy. Moreover, GEM combined therapy with IFN-α significantly suppressed xenograft tumor growth. In addition, $CD133^+$ cells showed CSC-like properties, such as generation of spheres in serum-free culture and tumorigenesis in NOD/SCID mice. Taken together, IFN-α, as a modulator, could contribute to the treatment of $CD133^+$ cancer cells with CSC-like properties and be effective in combined chemotherapies for pancreatic cancer stem-like cells.

Acknowledgment

This work was supported by grants-in-aid for scientific research from the Ministry of Education, Science, Sports, and Culture, Japan.

Disclosure Statement

The authors have no conflict of interest to declare.

References

1 Jemal A, Siegel R, Ward E, Hao Y, Xu J, Thun MJ. Cancer statistics, 2009. *CA Cancer J Clin* 2009; **59**: 225–49.
2 Reya T, Morrison SJ, Clarke MF, Weissman IL. Stem cells, cancer, and cancer stem cells. *Nature* 2001; **414**: 105–11.
3 Hanahan D, Weinberg RA. Hallmarks of cancer: the next generation. *Cell* 2011; **144**: 646–74.
4 Dean M. Cancer stem cells: implications for cancer causation and therapy resistance. *Discov Med* 2005; **5**: 278–82.
5 Eyler CE, Rich JN. Survival of the fittest: cancer stem cells in therapeutic resistance and angiogenesis. *J Clin Oncol* 2008; **26**: 2839–45.
6 Singh SK, Hawkins C, Clarke ID *et al.* Identification of human brain tumour initiating cells. *Nature* 2004; **432**: 396–401.
7 Beier D, Hau P, Proescholdt M *et al.* CD133(+) and CD133(−) glioblastoma-derived cancer stem cells show differential growth characteristics and molecular profiles. *Cancer Res* 2007; **67**: 4010–5.
8 Zhao P, Lu Y, Jiang X, Li X. Clinicopathological significance and prognostic value of CD133 expression in triple-negative breast carcinoma. *Cancer Sci* 2011; **102**: 1107–11.
9 Collins AT, Berry PA, Hyde C, Stower MJ, Maitland NJ. Prospective identification of tumorigenic prostate cancer stem cells. *Cancer Res* 2005; **65**: 10946–51.
10 Florek M, Haase M, Marzesco AM *et al.* Prominin-1/CD133, a neural and hematopoietic stem cell marker, is expressed in adult human differentiated cells and certain types of kidney cancer. *Cell Tissue Res* 2005; **319**: 15–26.
11 Ferrandina G, Bonanno G, Pierelli L *et al.* Expression of CD133-1 and CD133-2 in ovarian cancer. *Int J Gynecol Cancer* 2008; **18**: 506–14.
12 Zhu Z, Hao X, Yan M *et al.* Cancer stem/progenitor cells are highly enriched in CD133 + CD44 + population in hepatocellular carcinoma. *Int J Cancer* 2010; **126**: 2067–78.
13 O'Brien CA, Pollett A, Gallinger S, Dick JE. A human colon cancer cell capable of initiating tumour growth in immunodeficient mice. *Nature* 2007; **445**: 106–10.
14 Ricci-Vitiani L, Lombardi DG, Pilozzi E *et al.* Identification and expansion of human colon-cancer-initiating cells. *Nature* 2007; **445**: 111–5.
15 Haraguchi N, Ohkuma M, Sakashita H *et al.* CD133+ CD44+ population efficiently enriches colon cancer initiating cells. *Ann Surg Oncol* 2008; **15**: 2927–33.
16 Morikawa K, Okudo K, Haraguchi N *et al.* Combination use of anti-CD133 antibody and SSA lectin can effectively enrich cells with high tumorigenicity. *Cancer Sci* 2011; **102**: 1164–70.
17 Maeda S, Shinchi H, Kurahara H *et al.* CD133 expression is correlated with lymph node metastasis and vascular endothelial growth factor-C expression in pancreatic cancer. *Br J Cancer* 2008; **98**: 1389–97.
18 Hermann PC, Huber SL, Herrler T *et al.* Distinct populations of cancer stem cells determine tumor growth and metastatic activity in human pancreatic cancer. *Cell Stem Cell* 2007; **1**: 313–23.
19 Burris HA III, Moore MJ, Andersen J *et al.* Improvements in survival and clinical benefit with gemcitabine as first-line therapy for patients with advanced pancreas cancer: a randomized trial. *J Clin Oncol* 1997; **15**: 2403–13.
20 Stark GR, Kerr IM, Williams BRG, Silverman RH, Schreiber RD. How cells respond to interferons. *Ann Rev Biochem* 1998; **67**: 227–64.
21 Tagliaferri P, Caraglia M, Budillon A *et al.* New pharmacokinetic and pharmacodynamic tools for interferon-α (IFN-α) treatment of human cancer. *Cancer Immunol Immunother* 2005; **54**: 1–10.
22 Gresser I, Belardelli F. Endogenous type I interferons as a defense against tumors. *Cytokine Growth Factor Rev* 2002; **13**: 111–8.
23 Dunn GP, Koebel CM, Schreiber RD. Interferons, immunity and cancer immunoediting. *Nat Rev Immunol* 2006; **6**: 836–48.
24 Challen GA, Little MH. A side order of stem cells: the SP phenotype. *Stem Cells* 2006; **24**: 3–12.
25 Moserle L, Indraccolo S, Ghisi M *et al.* The side population of ovarian cancer cells is a primary target of IFN-α antitumor effects. *Cancer Res* 2008; **68**: 5658–68.
26 Solorzano CC, Hwang R, Baker CH *et al.* Administration of optimal biological dose and schedule of interferon alpha combined with gemcitabine induces apoptosis in tumor-associated endothelial cells and reduces growth of human pancreatic carcinoma implanted orthotopically in nude mice. *Clin Cancer Res* 2003; **9**: 1858–67.
27 Miyamoto A, Umeshita K, Sakon M *et al.* Advanced hepatocellular carcinoma with distant metastases, successfully treated by a combination therapy

of alpha-interferon and oral tegafur/uracil. *J Gastroenterol Hepatol* 2000; **15**: 1447–51.
28 Wada H, Nagano H, Yamamoto H *et al.* Combination therapy of interferon- and 5-fluorouracil inhibits tumor angiogenesis in human hepatocellular carcinoma cells by regulating vascular endothelial growth factor and angiopoietins. *Oncol Rep* 2007; **18**: 801–9.
29 Sparano JA, Lipsitz S, Wadler S *et al.* Phase II trial of prolonged continuous infusion of 5-fluorouracil and interferon-α in patients with advanced pancreatic cancer. Eastern Cooperative Oncology Group Protocol 3292. *Am J Clin Oncol* 1996; **19**: 546–51.
30 Wagener DJ, Wils JA, Kok TC, Planting A, Couvreur ML, Baron B. Results of a randomized phase II study of cisplatin plus 5-fluorouracjl versus cisplatin plus 5-fluorouracil with a-interferon in metastatic pancreatic cancer. An EORTC gastrointestinal tract cancer group trial. *Eur J Cancer* 2002; **38**: 648–53.
31 Martínez CC, Alvarez SN, Vicente OV, García RJ, Pascual CF, Campos AM. In vitro and in vivo effect of IFN-αlpha on B16F10 melanoma in two models: subcutaneous (C57BL6J mice) and lung metastasis (Swiss mice). *Biomed Pharmacother* 2009; **63**: 305–12.
32 Hertel LW, Boder GB, Kroin JS *et al.* Evaluation of the antitumor activity of gemcitabine (2′,2′-difluoro-2′-deoxycytidine). *Cancer Res* 1990; **50**: 4417–22.
33 Essers MA, Offner S, Blanco Bose WE *et al.* IFNα activates dormant haematopoietic stem cells in vivo. *Nature* 2009; **458**: 904–8.
34 Persano L, Moserle L, Esposito G *et al.* Interferon-alpha counteracts the angiogenic switch and reduces tumor cell proliferation in a spontaneous model of prostatic cancer. *Carcinogenesis* 2009; **30**: 851–60.
35 Joshi S, Kaur S, Redig AJ *et al.* Type 1 interferon (IFN)-dependent activation of Mnk1 and its role in the generation of growth inhibitory responses. *Proc Natl Acad Sci USA* 2009; **106**: 12097–102.
36 Hirschmann-Jax C, Foster AE, Wulf GG *et al.* A distinct "side population" of cells with high drug efflux capacity in human tumor cells. *Proc Natl Acad Sci USA* 2004; **101**: 14228–33.
37 Kondo T, Setoguchi T, Taga T. Persistence of a small subpopulation of cancer stem-like cells in the C6 glioma cell line. *Proc Natl Acad Sci USA* 2004; **101**: 781–6.
38 Chiba T, Kita K, Zheng YW *et al.* Side population purified from hepatocellular carcinoma cells harbors cancer stem cell-like properties. *Hepatology* 2006; **44**: 240–51.
39 Haraguchi N, Utsunomiya T, Inoue H *et al.* Characterization of a side population of cancer cells from human gastrointestinal system. *Stem Cells* 2006; **24**: 506–13.
40 Lim R, Knight B, Patel K, McHutchison JG, Yeoh GC, Olynyk JK. Antiproliferative effects of interferon alpha on hepatic progenitor cells in vitro and in vivo. *Hepatology* 2006; **43**: 1074–83.
41 Mueller MT, Hermann PC, Witthauer J *et al.* Combined targeted treatment to eliminate tumorigenic cancer stem cells in human pancreatic cancer. *Gastroenterology* 2009; **137**: 1102–13.

Supporting Information

Additional Supporting Information may be found in the online version of this article:

Fig. S1. Flow cytometric analysis of cell cycle progression in Capan-1 cells treated with gemcitabine (100 ng/mL) for 12 or 24 h.

Fig. S2. Flow cytometric analysis of CD133 expression in Capan-1 cells treated with or without interferon-alpha (IFN-α). IFN-α treatment (5000 IU/mL) for 24 h decreased the ratio of $CD133^+$ Capan-1 cells over time.

Fig. S3. Comparison of BrdU assay between $CD133^+$ and $CD133^-$ Capan-1 cells treated with gemcitabine (GEM) (100 ng/mL) alone, interferon-alpha (IFN-α) (5000 U/mL) alone or GEM combined with IFN-α for 24 h.

Fig. S4. (A) Body weight curves of nude mice were not significantly different among the three treatments, which were gemcitabine (GEM) (100 ng/mL) alone, interferon-alpha (IFN-α) (5000 U/mL) alone or GEM plus IFN-α. (B) Comparison of proportions of $CD133^+$ cells in Capan-1 xenografts that were treated with GEM (100 ng/mL) alone, IFN-α (5000 U/mL) alone or GEM plus IFN-α at week 2 and 5.

Fig. S5. (A) Comparison of the number of spheres per well (cm^3) for pancreatic cancer cell lines, Panc-1, Capan-1, MIA PaCa-2, PK45H and SW1990. The white and black bars indicate the spheres composed of 3–30 and >30 cells, respectively. (B) Immunohistochemical study of a Capan-1 tumor generated by transplantation into non-obese diabetic (NOD)/SCID mice. (i) HE staining and (ii, iii, iv) immunostaining performed to identify cytokeratin (CK) and CD133 expression, respectively.

Table S1. Comparison of potential markers related to tumor-initiating cells in six pancreatic cancer cell lines.

Please note: Wiley-Blackwell are not responsible for the content or functionality of any supporting materials supplied by the authors. Any queries (other than missing material) should be directed to the corresponding author for the article.

doi: 10.1111/j.1349-7006.2012.02235.x

Human Cell (2012) 25:1–8
DOI 10.1007/s13577-011-0037-9

RESEARCH ARTICLE

Establishment of a highly migratory subclone reveals that CD133 contributes to migration and invasion through epithelial–mesenchymal transition in pancreatic cancer

Qiang Ding · Makoto Yoshimitsu · Taisaku Kuwahata · Koki Maeda · Tomomi Hayashi · Toru Obara · Yumi Miyazaki · Shyuichiro Matsubara · Shoji Natsugoe · Sonshin Takao

Received: 25 July 2011 / Accepted: 20 October 2011 / Published online: 23 November 2011

Abstract Pancreatic cancer is a lethal disease because of invasion and early metastasis. Although CD133, a marker of cancer stem cells (CSCs) in a variety of solid tumors, has been studied in recent decades, its function remains obscure. Recent reports suggest that epithelial–mesenchymal transition (EMT) may be related to the properties of CSCs. In this study, we investigated whether CSC markers are associated with EMT. For Capan1M9, a highly migratory cell subclone established from human pancreatic cancer cell line Capan-1, CD133 expression, migration, and invasion were greater than for the parent cells. In Capan1M9 cells, the EMT-related transcription factors Slug and Snail were up-regulated, and N-cadherin and fibronectin were also substantially increased. In contrast, occludin and desmoplakin were suppressed. Knockdown of endogenous CD133 in the Capan1M9 cells led to Slug suppression and reduction of migration and invasion. Taken together, CD133 has an important role in migration and invasion by facilitating EMT in pancreatic cancer cells.

Keywords Epithelial–mesenchymal transition (EMT) · CD133 · Migration · Slug · Pancreatic cancer

Electronic supplementary material The online version of this article (doi:10.1007/s13577-011-0037-9) contains supplementary material, which is available to authorized users.

Q. Ding · T. Kuwahata · K. Maeda · T. Obara · Y. Miyazaki · S. Matsubara · S. Takao (✉)
Division of Cancer and Regenerative Medicine, Frontier Science Research Center, Kagoshima University Graduate School of Medical and Dental Sciences, 8-35-1 Sakuragaoka, Kagoshima 890-8520, Japan
e-mail: sonshin@m2.kufm.kagoshima-u.ac.jp

M. Yoshimitsu
Department of Hematology and Immunology, Kagoshima University Graduate School of Medical and Dental Sciences, 8-35-1 Sakuragaoka, Kagoshima 890-8520, Japan

K. Maeda · T. Hayashi · S. Natsugoe
Department of Digestive Surgery, Kagoshima University Graduate School of Medical and Dental Sciences, 8-35-1 Sakuragaoka, Kagoshima 890-8520, Japan

Introduction

Pancreatic cancer is an exceptionally devastating and incurable disease because of early local invasion and distant metastasis to the lymph nodes and liver [1]. Most pancreatic cancers at diagnosis are advanced and unresectable, and very little effective therapy can currently be offered to patients. Therefore, it is critical to understand the molecular mechanism of invasion and metastasis [2].

Metastasis involves several processes, including cancer cell detachment from the primary tumor, local invasion, dissemination through surrounding blood vessels or lymphatic vessels, and attachment and proliferation at the metastatic site [3]. Although metastasis is a complicated process involving multiple factors and genetic events, increased migratory and invasive capabilities are critical to initiation of the process [4, 5]. During cancer progression, some cells within the primary tumor may reactivate a latent embryonic program known as epithelial–mesenchymal transition (EMT), thereby acquiring increased motility and invasiveness; this facilitates invasion of both local and distant tissues by cancerous cells [6]. During EMT, cells lose their epithelial characteristics, including cell adhesion and polarity [7, 8], and acquire a mesenchymal morphology and the ability to migrate. EMT is a recognized mechanism for dispersing cells during embryonic development [9], tissue regeneration [10], and initiation of invasive and metastatic

behavior in epithelial cancer [11–13]. Local invasion is believed to be an initial and essential step leading to the generation of usually fatal distant metastases [3, 11].

CD133 (prominin-1) is a cell membrane protein first found in hematopoietic stem cells and early progenitor cells in the bone marrow [14]. It has recently been used extensively as a marker to identify stem cells from normal and cancerous tissue [15–17]. However, evidence also suggests that CD133 expression is not restricted to cancer stem cells (CSCs). For example, in rat glioma cell line C6, both $CD133^+$ and $CD133^-$ subpopulations had clonogenic, self-renewal, and tumorigenic capacity [18]. Several signaling pathways have been shown to regulate CD133 epitope-positive cells. For example, the Notch, Hedgehog, and bone morphogenic protein (BMP) signaling pathways have been shown to be dependent on the tissue-specific expression of splice variants of prominin-family molecules [17, 19]. Taken together, these data suggest that further investigation is still needed to understand the biological role of CD133 in cancer development.

We have previously reported a significant correlation between CD133 expression and clinicopathologic factors, histological type, lymphatic invasion, and lymph node metastasis in patients with pancreatic cancer who underwent a curative operation [2]. Therefore, it is plausible that CD133 is involved in migration and invasion. Because EMT consists of sequential multistep programs during tumor metastasis, an appropriate method or in-vitro cell line is needed for further elucidation of this complicated program. In this study, a highly migratory and invasive cell line was established from the pancreatic cancer cell line, Capan-1, to investigate the mechanism involved in migration and to identify further promising targets for preventing metastasis.

Materials and methods

Cell culture

Human pancreatic cancer cell line, Capan-1, was purchased from the American Type Culture Collection (ATCC, VA, USA) and cultured in DMEM/F12 (Sigma, MO, USA) medium containing 10% fetal bovine serum (FBS; Invitrogen, CA, USA) supplemented with 100 units/ml penicillin and 100 mg/ml streptomycin, followed by incubation at 37°C under a humidified atmosphere containing 5% CO_2. Cell growth rate was examined by cell counting.

Selection of migratory subclones from the Capan-1 cell line

Figure 1 outlines the procedure used for selecting the migratory subclones. Cells (2×10^5) suspended in serum-free medium were seeded into a single well of a 24-well cell-culture insert (8.0 μm pore size), and the insert was placed into plates containing 10% FBS as chemoattractant. The plate was incubated for 18 h at 37°C in 5% CO_2. Migrating cells were collected from the underside of the membrane by use of Accutase™ (Millipore, MA, USA), seeded into the 24-well plate again, and expanded into a 35 cm^2 flask; these cells were designated Capan1M1. When the selected cells were confluent, an aliquot (5×10^4 cells/well) was applied to another migration insert and migrating cells were collected as described above. In total, the procedure was repeated 9 times, and two to threefold repeatable differences in migration and invasion were achieved.

Migration and invasion assays

Cells ($2–5 \times 10^4$) were seeded, in serum-free medium, into 24-well BD Falcon migration inserts (8 μm pore size) for migration or into a BD BioCoat Matrigel invasion chamber (BD Biosciences, NJ, USA). Inserts were placed into plates containing 10% FBS as chemoattractant and incubated for 18 h for migration and 24 h for invasion. After incubation, media plus cells were removed from the top chamber by use of cotton swabs and phosphate-buffered saline (PBS). The membrane with cells was stained with Giemsa for 5 min. The number of migrating or invading cells in 10 fields was counted at 20× magnification by light microscopy. Data were calculated as mean ± SD.

Wound-healing assay

CytoSelect™ 24-well wound-healing assay (Cell Biolabs, CA, USA) was used as the migration assay. Wound field was generated according to the product manual. Cell sus-

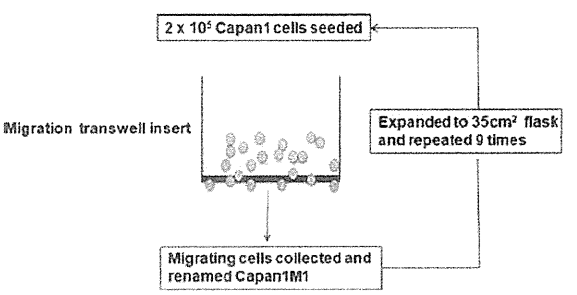

Fig. 1 Selection of Capan1M9 migratory subclone by use of the migration transwell insert. For the first round of selection a total of 2×10^5 Capan-1 parental cells were seeded into a 24-well migration transwell insert and incubated for 18 h. Migrating cells were collected from the bottom of the membrane by use of Accutase™, plated into the 24-well plate, expanded into a 35 cm^2 flask, and renamed Capan1M1. When confluent, the cells were subjected to further rounds of selection by repeating the migration assay. In total, the procedure was repeated 9 times and the cells were designated Capan1M9

pension was added to the well with the insert in place then incubated for 24–48 h. The cells were then cultured until a monolayer formed and the insert was removed to generate a "wound field". Cells were monitored, under a microscope, for migration into the wound field until the wound closed. Wound-healing area was calculated by use of Axiovision Rel software (Zeiss, Germany).

Immunofluorescence staining

Immunofluorescence staining was performed on primary adherent cultures of Capan-1 cells. After fixing with 10% formalin the cells were incubated with primary antibody staining for 2 h in an incubator at 37°C with anti-E-cadherin and vimentin (Santa Cruz, CA, USA) then washed three times with PBS and 2% FBS. This was followed by incubation for 1 h with Alexa Fluor® goat anti-mouse secondary antibody (Invitrogen). DAPI nuclear staining was performed for a further 5 min and an additional three washes. These stained cells were viewed by fluorescent microscopy (Zeiss). Primary antibodies were replaced by PBS in the negative control group.

Cell lysis and immunoblotting

Cells were lysed on ice in lysis buffer and the lysates were boiled for 5 min, clarified by centrifugation at 15000*g* for 15 min, and separated by SDS-PAGE. The proteins were transferred on to nitrocellulose membranes. The membranes were incubated with a 1:100–200 dilution of the following human polyclonal or monoclonal antibodies: E-cadherin, vimentin, N-cadherin, Slug (Santa Cruz), fibronectin (R&D, MN, USA), desmoplakin, occludin, Snail (Abcam, MA, USA), and CD133 (Miltenyi Biotec, Germany) followed by 1:200–1000 dilution of peroxidase-conjugated anti-goat IgG, anti-rabbit IgG (Santa Cruz) or anti-mouse IgG (Jackson Immunoresearch, PA, USA) antibody for the secondary reaction. As an internal control for the amount of protein loaded, β-actin was detected by use of a specific antibody (Sigma). The immunocomplex was visualized by use of the ECL Western blot detection system (Amersham, UK).

Real-time quantitative RT-PCR (ABI)

Total RNA (tRNA) was extracted by use of an RNeasy extraction kit (Qiagen, Germany). Primers and probes were obtained from Applied Biosystems™ (Life Technologies, CA, USA) as Assay-on-Demand Gene Expression Products. Real-time RT-PCRs were conducted in accordance with the supplier's directions. PCR mixture (20 µl) contained 10 µl 2× Taqman Universal PCR Master Mix, 1 µl 20× working stock of gene expression assay mix, and 20 µg tRNA. Real-time RT-PCRs were done in a StepOne Real-time PCR system (Applied Biosystems, CA, USA). The reaction for each sample was conducted in triplicate. Fluorescence of the PCR products was detected by use of the same apparatus. The number of cycles for the amplification plot to reach the threshold limit (C_t value) was used for quantification. Glyceraldehyde-3-phosphate dehydrogenase (GAPDH) was used for normalization.

Capan1M9-GFP-shCD133 cell line established by lentiviral transduction

pLVTHM is a second-generation lentiviral vector which engineers shRNA under H1 promoter (Addgene, MA, USA) and co-expresses enGFP under the elongation factor 1α promoter. CD133 shRNA 877 sense (5′-cgcgtccccggacaaggcgttcacagatttcaagagaatctgtgaacgccttgtccttttttggaaat-3′) and CD133 shRNA 877 antisense (5′-cgatttccaaaaaggacaaggcgttcacagattctcttgaaatctgtgaacgccttgtccgggga-3) oligonucleotides were annealed to each other and ligated into the pLVTHM vector at the *Cla*I and *Mlu*I sites, which yields pLVTHM-CD133-877 shRNA transfer vector. 293T cells were co-transfected with 4 µg pLVTHM-CD133-877 shRNA transfer plasmid, 3 µg psPAX2 packaging plasmid, and 1 µg pMD2.G envelope plasmid by use of Fugene 6 transfection reagent (Roche, CA, USA). Twenty-four hours after transfection the medium was replaced with fresh DMEM + 10% FBS. Forty-eight hours after transfection, viral supernatant was harvested and filtered through a 0.45-µm filter. Capan1M9 cells expressing CD133 were transduced with filtered viral supernatant containing 8 µg/ml protamine sulfate 72 h after transfection. Flow-cytometric analysis was performed with a FACSCan (BD Biosciences, CA, USA) for enGFP expression. enGFP-positive cell fractions were then sorted by use of a FACSAria (BD Biosciences). The purity of the fractions routinely exceeded 95%. CD133-PE, CD44-APC, and CD24-FITC antibody (Miltenyi, Germany) were used for flow-cytometric analysis.

Statistical analysis

Group differences were analyzed statistically by use of Student's t test ($p < 0.05$ was considered statistically significant) in StatView statistical software version 5.0 (SAS Institute, NC, USA).

Results

Selection of a migratory subclone, Capan1M9, from the Capan-1 parental cell line

For cultured Capan-1 cells, tightly packed clusters in a monolayer growth pattern and a variety of cell shapes were